THE CAROTENOID CLEAVAGE DIOXYGENASES OF *ARABIDOPSIS THALIANA*

By

MICHELE ELENA AULDRIDGE

A DISSERTATION PRESENTED TO THE GRADUATE SCHOOL
OF THE UNIVERSITY OF FLORIDA IN PARTIAL FULFILLMENT
OF THE REQUIREMENTS FOR THE DEGREE OF
DOCTOR OF PHILOSOPHY

UNIVERSITY OF FLORIDA

2004

I dedicate this work to my parents who support me in every decision that I make.

ACKNOWLEDGMENTS

I would like to thank my advisor, Harry J. Klee, whose consistent belief in me made this possible, and my committee members, Donald McCarty, Andrew Hanson, and Steve Talcott for their critical advice. I am grateful for the assistance of Carole Dabney-Smith for work with chloroplast import, Eric Schmelz with hormone and ionone analysis and Anna Block for assistance with plant measurements and support with my project. I would also like to thank my parents for their love and support and Brian Burger who gave me the confidence and encouragement to get me through to the end.

TABLE OF CONTENTS

page

LIST OF TABLES

LIST OF FIGURES

Abstract of Dissertation Presented to the Graduate School
of the University of Florida in Partial Fulfillment of the
Requirements for the Degree of Doctor of Philosophy

THE CAROTENOID CLEAVAGE DIOXYGENASES OF *ARABIDOPSIS THALIANA*

By

Michele Elena Auldridge

December 2004

Chair: Harry J. Klee
Major Department: Plant Molecular and Cellular Biology

Dioxygenases are critical players in essential metabolic pathways in both plants and animals. Several subclasses of dioxygenases exist, one of which is the recently discovered Carotenoid Cleavage Dioxygenase (CCD) family that has been most studied in the plant species *Arabidopsis thaliana*. Arabidopsis has nine CCDs, identified because of their similarity to the maize VP14 enzyme. *VP14* was the first CCD cloned and is involved in the production of the phytohormone abscisic acid. Five of the Arabidopsis dioxygenases are involved in ABA biosynthesis. The remaining four family members seem less likely to be involved in ABA biosynthesis because of their sequence divergence from VP14.

Here, three of the Arabidopsis CCDs, *CCD1*, *7* and *8*, were characterized biochemically and genetically. *In vitro* assays have confirmed the identification of CCD1 and CCD7 as carotenoid dioxygenases by demonstrating their capacity to cleave a variety of carotenoids. CCD8 possesses activity on one of the apocarotenoids resulting from

CCD7's activity on β-carotene. Despite its confirmed activity on carotenoids, CCD1 was not localized to the plastid, whereas CCD7 and CCD8 were plastid localized. Loss-of-function mutants were isolated for each CCD studied and their associated phenotypes were analyzed. The *CCD1* mutants showed a decrease in petiole and leaf blade lengths but were like wild-type in all other aspects of growth and development. *CCD7* and *CCD8* mutants exhibited identical phenotypes consisting of decreased petiole and leaf blade lengths and an increased branching pattern, found to be independent of the synthesis of auxin and abscisic acid (ABA). CCD7 and CCD8 are involved in the biosynthesis of a novel signaling molecule, which controls branching in Arabidopsis. The signaling molecule has not yet been identified but is derived from a carotenoid backbone by the sequential action of CCD7 and CCD8 activity.

CHAPTER 1
INTRODUCTION

Carotenoid Cleavage Dioxygenase Family

Recently a new class of dioxygenases, Carotenoid Cleavage Dioxygenases (CCD), was discovered, with representatives found in both the plant and animal kingdoms. The first gene encoding a carotenoid cleavage dioxygenase was isolated from the maize abscisic acid deficient, viviparous mutant, *vp14*. *VP14* encodes a CCD that catalyzes the first step in abscisic acid (ABA) biosynthesis. ABA is a plant hormone necessary for resistance to drought and is also involved in dormancy such that mutants which lack appropriate ABA concentrations and/or sensitivity to ABA germinate precociously (Finkelstein et al., 2002). The members of this new family of dioxygenases share several characteristics: they contain five conserved histidines spread throughout their primary protein sequence, they all require Fe^{2+} ions thought to be coordinated by the five histidine residues (Schwartz et al., 1997; Kiefer et al., 2001; Redmond et al., 2001), and they all contain a conserved polypeptide segment at their carboxy terminus that minimally constitutes a signature sequence for the family (Fig. 1-1A) (Redmond et al., 2001). Mechanistically, all CCDs of plant and animal origin are presumed to act similarly in that they incorporate both oxygen atoms from molecular oxygen into their substrates across a double bond resulting in the production of two aldehyde-containing cleavage products. The double bond broken is that of a carotenoid molecule and the resulting products are aldehyde-containing terpenoid compounds, called apocarotenoids.

A.

```
HsDIOXI     EDDGVIL
HsDIOXII    EDGGVIL
AtCCD8      EDDGVVI
HsRPE65     EDDGVVL
AtCCD1      EDDGYLI
AtCCD7      EDDGYIV
AtNCED3     EDEGYIL
```

B.

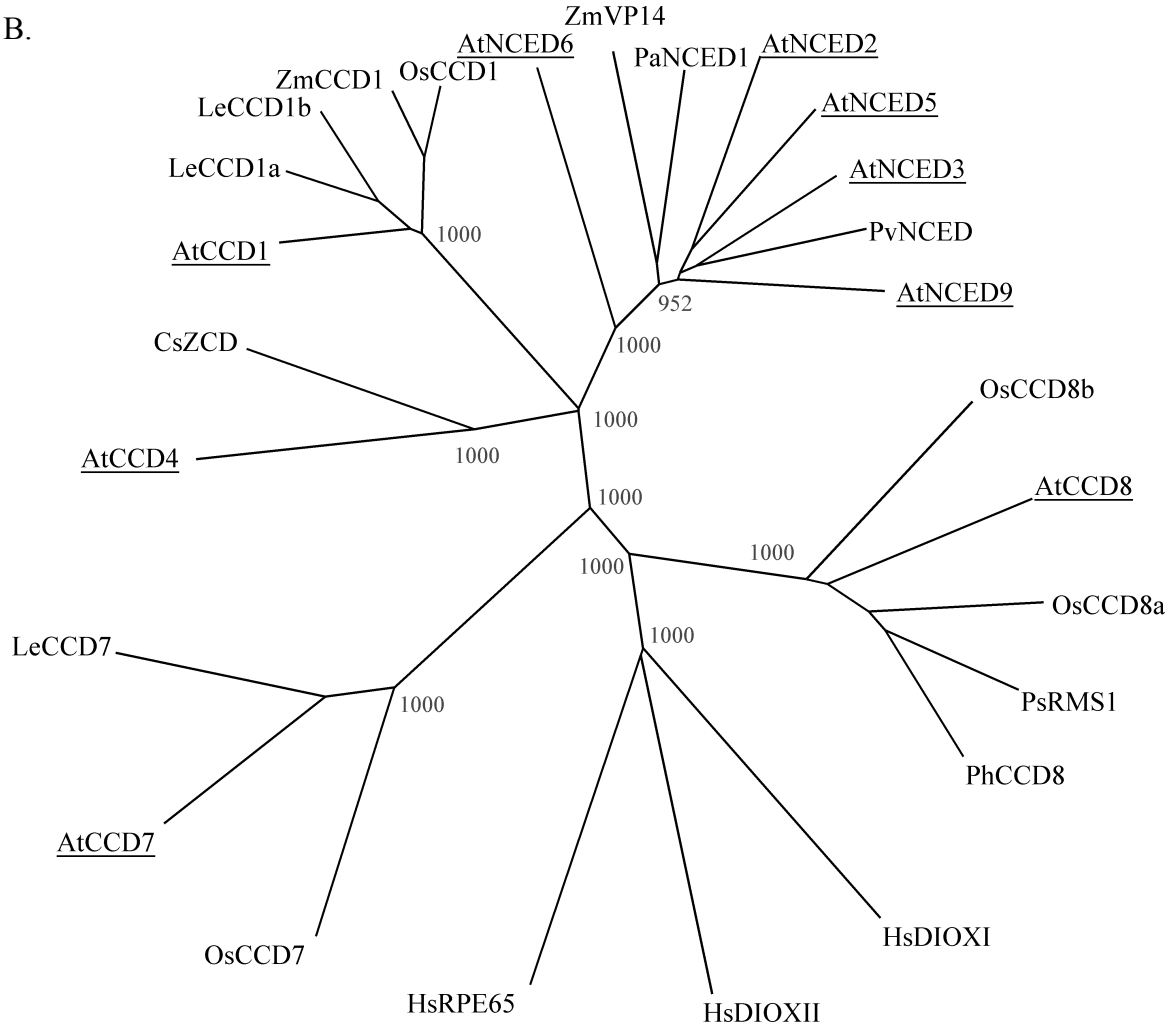

Figure 1-1 The Carotenoid Cleavage Dioxygenase (CCD) family. A) Conserved region at the carboxy terminus of all CCD family members. Four members from Arabidopsis (CCD1, NCED3, CCD7, and CCD8) and three from human (β-dioxI, β-dioxII, and RPE65) are shown. B) Phylogenetic tree of representative members from maize, avocado, bean, crocus, rice, pea, petunia, tomato and human. All Arabidopsis members (underlined) identified to date are shown. Alignment and phylogenetic tree were created with ClustalX and TreeView. Numbers at major nodes of tree are bootstrap values out of 1000 bootstrap trials and represent a confidence level for each grouping.

CCDs have been found in several plant species including tomato (Burbidge et al., 1999; Simkin et al., 2004a), bean (Qin and Zeevaart, 1999), cowpea (Iuchi et al., 2000), avocado (Chernys and Zeevaart, 2000), bixa (Bouvier et al., 2003a), crocus (Bouvier et al., 2003b), and petunia (Simkin et al., 2004b). They have also been identified in drosophila, mouse, zebrafish and humans (von Lintig and Vogt, 2000; Kiefer et al., 2001; Redmond et al., 2001; Lindqvist and Andersson, 2002). *Arabidopsis thaliana* is a representative species for study of the CCD family because the entire family has been identified and many members have been well characterized both genetically and biochemically (Schwartz et al., 2001; Tan et al., 2003; Booker et al., 2004). Based on sequence homology to VP14, nine putative CCDs have been identified in the Arabidopsis genome. Figure 1-1B shows a phylogenetic tree containing the Arabidopsis CCDs. This tree illustrates the divergence found within the Arabidopsis CCD family. Five of the members group with the maize protein VP14, whereas the remaining four members are less similar to VP14. The CCD family members in Arabidopsis are listed in Table 1-1 along with their accession numbers, chromosome locations, and gene identifications. The family is divided into two groups, the carotenoid cleavage dioxygenases (CCDs) and the

Table 1-1. The CCD Gene Family of Arabidopsis

Gene	Accession	Chromosome	Gene ID
AtCCD1	AJ005813	3	At3g63520
AtNCED2	AL021710	4	At4g18350
AtNCED3	AB028617	3	At3g14440
AtCCD4	AL021687	4	At4g19170
AtNCED5	AC074176	1	At1g30100
AtNCED6	AB028621	3	At3g24220
AtCCD7	AC007659	2	At2g44990
AtCCD8	AL161582	4	At4g32810
AtNCED9	AC013430	1	At1g78390

9-cis-epoxycarotenoid dioxygenases (NCEDs). These designations refer to the substrate preference of the enzyme.

In this work, three members (CCD1, CCD7, and CCD8) of the CCD family in Arabidopsis are studied both molecularly and genetically. These three members were chosen for study because of their significant divergence from the remaining members in gene structure and sequence homology to VP14 (Table 1-2). CCD4 was originally thought to belong to the NCED subgroup in the CCD family mostly due to its gene structure and was not included in the present study. However, recent biochemical studies show that it belongs to the CCD subgroup (see Activity section in this chapter).

Table 1-2. Comparison of the CCD and NCED gene structures and identities to VP14.

Family Member	Intron #	% Identity to VP14
AtCCD1	**13**	**37**
AtNCED2	0	64
AtNCED3	0	67
AtCCD4	0	41
AtNCED5	0	66
AtNCED6	0	57
AtCCD7	**5**	**21**
AtCCD8	**5**	**26**
AtNCED9	0	67

Carotenoids

The dioxygenases discussed here use carotenoids as substrates. Therefore, a brief discussion on carotenoid biosynthesis, function, and location within the cell is appropriate. Carotenoids are C_{40} compounds, with a series of conjugated double bonds, produced in the plastids of plants. The condensation of two geranylgeranyl diphosphate molecules to form phytoene is the first committed step in the carotenoid biosynthetic pathway (Fig. 1-2). Geranylgeranyl diphosphate is a C_{20} compound formed from the sequential addition of three molecules of the 5 carbon compound isopentenyl

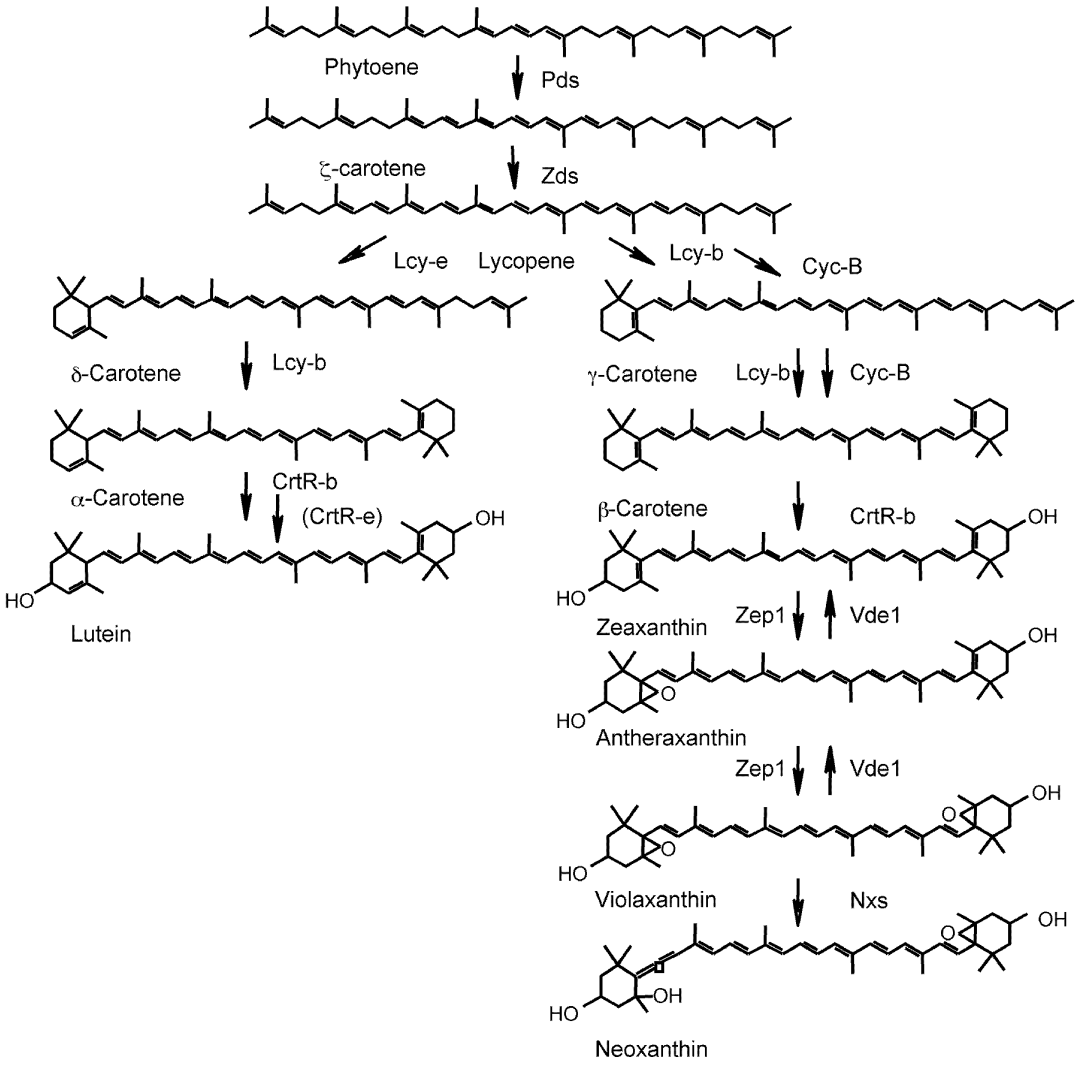

Figure 1-2. Carotenoid biosynthetic pathway. Abbreviations are as follows; Pds, phytoene desaturase; Zds, -carotene desaturase; Lcy-e, lycopene -cyclase; Lyc-b, lycopene -cyclase; CrtR-b, -ring hydroxylase; CrtR-e, -ring hydroxylase;, Zep1, zeaxanthin epoxidase; Vde1, violaxanthin de-epoxidase; Nxs, neoxanthin synthase . Adapted from (Hirschberg, 2001).

pyrophosphate (IPP) to its isomer dimethylallyl diphosphate (DMADP). IPP is the basic component of all isoprenoid compounds, including such diverse plant metabolites as cytokinins, chlorophylls, gibberellins, sesquiterpenes and sterols (Cunningham and Gantt, 1998). There are two pathways leading to the synthesis of IPP, the cytosolic acetate/mevalonate (MVA) pathway and the plastid localized 1-deoxy-D-xylulose-5-phosphate (DOXP) pathway. In higher plants, sterols and sesquiterpenes are made up of

IPP molecules formed via the MVA pathway in the cytosol, whereas carotenoids, cytokinins, chlorophylls and gibberellins consist of IPP molecules formed via the DOXP pathway in the plastid (Lichtenthaler, 1999).

The formation of phytoene is followed by several desaturation steps, resulting in synthesis of the linear carotenoid lycopene. The cyclic carotenoids are produced through the sequential cyclization of lycopene's ends. Some carotenoid molecules contain oxygen as a consequence of subsequent hydroxylation and/or epoxidation reactions. These carotenoids are called xanthophylls. It has been hypothesized that the enzymes involved in carotenoid biosynthesis are part of a multi-enzyme complex associated with the thylakoid membrane (Cunningham and Gantt, 1998). A multi-enzyme complex would allow for concomitant regulation of the pathway, with each of its components being dependent on functional operation of the other components. This also would decrease the substrate available for degradation if, once the carotenoid precursors are fed into the complex, they do not emerge until formed into the carotenoid dictated by the final enzyme. If this were so, the substrates available for cleavage by dioxygenases would be tightly regulated.

Carotenoids have two main functions in photosynthesis. Because of their system of conjugated double bonds, they are able to absorb energy from photons. The number of double bonds dictates the maximum absorption of the carotenoid molecule. The absorption maxima range from 400 to 500nm. Carotenoids are able to absorb energy from sunlight and pass it on to nearby chlorophyll molecules to be used in photosynthesis. In this way, they act as accessory pigments to chlorophyll and are part of the light harvesting complexes associated with the photosystems within the thylakoid

membranes. They are also able to accept energy from excited triplet state chlorophyll molecules. If carotenoids were not present to receive this energy from the overly excited chlorophyll molecules, formation of singlet state oxygen radicals could result (van den Berg, 2000). Depending on the light environment, it may be necessary to adjust the carotenoid content of the photosystems. CCDs may degrade photosynthetic carotenoids in order to achieve the optimal carotenoid content necessary for a particular light environment.

Carotenoids are also thought to function as membrane stabilizers. In general the thylakoid membranes are fairly fluid. This fluidity allows movement of the photosystems and light harvesting complexes, which is essential for maximizing photosynthesis and minimizing photo-oxidative damage in different light conditions. Most carotenoids found within the thylakoid membranes are associated with the light harvesting complexes. However, there are some carotenoids that are not, and may instead act to rigidify the thylakoid membrane. High solar irradiances are usually associated with increased heat. An increase in temperature can cause disorganization of lipid bilayers, allowing for breakdown of protein complexes such as those found in the photosystems and light harvesting complexes. Therefore, an increase in the concentration of stabilizing carotenoids in membranes could protect the thylakoid membranes during periods of increased solar irradiance. One carotenoid implicated in this process is zeaxanthin. With its polar hydroxyl groups at each end of the molecule, zeaxanthin inserts itself almost perpendicular to the thylakoid membrane, acting to decrease membrane fluidity (Havaux, 1998). A possible function of carotenoid cleavage dioxygenases in regulating membrane fluidity could be envisioned. *In vitro*, all-*trans*-zeaxanthin is a possible substrate for

AtCCD1 (Schwartz et al., 2001). The action of a CCD could facilitate the xanthophyll cycle in zeaxanthin turnover resulting in a quick increase in membrane fluidity. Localization of the CCDs, not only within the plastid but also in association with the thylakoid membranes, will be integral in determining whether this function is a possibility *in vivo*.

Apocarotenoids

Products resulting from the degradation of a carotenoid at any of its double bonds are called apocarotenoids. To date, many apocarotenoids and, in some cases, the dioxygenases responsible for their production have been identified in plants and animals. Five major sites of cleavage are illustrated in Figure 1-3 by arrows pointing to the 7,8, 9,10, 11,12, 13,14 and 15,15' double bonds of β-carotene. Alternatively, owing to the symmetrical nature of carotenoid molecules, cleavage can also occur at the 7',8', 9',10', 11',12' and 13',14' double bonds. Several examples of apocarotenoids are discussed below with respect to the carotenoid precursor and the site of its cleavage.

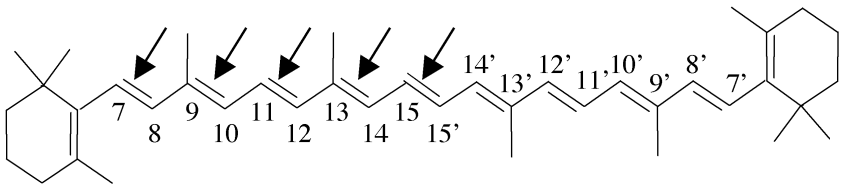

Figure 1-3. β-carotene with its major sites of cleavage indicated by arrows.

The most accessible double bonds of β-carotene to cleavage are numbered in Figure 1-3. However in linear carotenoids such as lycopene the 5,6 (5',6') double bond is open for attack by a dioxygenase. Such is the case for the reaction at the start of bixin biosynthesis (Bouvier et al., 2003a). Bixin is an apocarotenoid that is a valued food colorant. Cleavage at the 7,8 (7',8') double bond of zeaxanthin leads to the production of

safranal, the most abundant constituent of saffron flavor (Bouvier et al., 2003b). Cyclic C_{13} apocarotenoids result from cleavage at the 9,10 (9',10') double bond of carotenoids with cyclized ends. Due to their volatile nature, these C_{13} apocarotenoids are constituents of the flavor and aroma of various fruits and vegetables. They include ionone derivatives (found in rose, tomato, tea), theaspirone (found in tea), and α-damascenone (found in wine, rose, tomato) (Winterhalter and Rouseff, 2002). Interestingly, ß-ionone, formed by cleavage of ß-carotene, has been shown to have antifungal activities (Fester, 1999). Asymmetric cleavage of a carotenoid molecule at its 9,10 double bond produces both C_{13} and C_{27} apocarotenoids. An example of a C_{27} apocarotenoid is the biologically active retinoic acid. In animals, retinoic acid regulates gene expression through its binding to two types of nuclear receptors, retinoic acid receptors (RARs) and retinoid X receptors (RXRs) (Mangelsdorf et al., 1993). In plants, cleavage at the 11,12 position (or 11',12' depending on carotenoid substrate) of 9-cis epoxycarotenoids produces xanthoxin, which is the precursor to the plant hormone ABA (Schwartz et al., 1997; Tan et al., 1997). Apocarotenoids resulting from cleavage at the 13,14 (13',14') double bond have not been reported. However, further cleavage of an apocarotenoid at this double bond was demonstrated for the Arabidopsis CCD8 enzyme (For further details, see next section as well as Chapter 4). Finally, central cleavage at the 15,15' double bond breaks the carotenoid molecule in half. With β-carotene as a substrate, central cleavage gives rise to two molecules of retinal (C_{20}). Retinal interacts with the protein opsin in the eye and acts as the visual chromophore making vision possible (Saari, 1994).

Carotenoid Cleavage Dioxygenase Activity in Arabidopsis

The members of the CCD family in Arabidopsis share the sequence characteristics found in all CCDs but they diverge into two groups, the NCEDs and the CCDs, based on their characterized or inferred substrate preference. The acronym NCED refers to the substrate, 9-*cis*-epoxycarotenoid, which is the preferred substrate for these dioxygenases. Figure 1-4 summarizes the enzymatic activity associated with all of the Arabidopsis CCDs.

VP14 belongs to the NCED group. It acts specifically at the 11,12 double bond of either of two 9-cis-epoxycarotenoids, violaxanthin or neoxanthin, to produce xanthoxin, the precursor to ABA (Schwartz et al., 1997). Four of the nine Arabidopsis dioxygenases (NCED2, NCED3, NCED6, and NCED9) have been shown to possess the same activity as VP14 and are designated NCEDs (Iuchi et al., 2001). NCED5 displays high sequence homology to VP14, however its activity has yet to be determined. The remaining four proteins diverge from the family and have been given the general designation of CCD. Two of the CCDs, CCD1 (see Chapter 2) (Schwartz et al., 2001) and CCD7 (see Chapter 3) (Booker et al., 2004), have been shown to cleave various substrates. They do, however, cleave their substrates specifically at the 9,10 double bond. They differ in that CCD1 cleaves its substrates symmetrically, whereas CCD7 cleaves asymmetrically (Schwartz et al., 2004). For example with β-carotene as a substrate, CCD1 produces two C_{13} products (both β-ionone) and one central C_{14} dialdehyde. Conversely, CCD7 produces one β-ionone product and the C_{27} product, 10'-apo-β-carotenal. A possible explanation for this distinct set of cleavage reactions is that CCD1 acts as a dimeric protein (Schwartz et al., 2001). CCD4 has yet to be biochemically characterized.

However, apocarotenoids such as 6-methyl-5-heptene-2-one have been found in tomato (Baldwin, 2000) and apple (Cunningham, 1986). These apocarotenoids result from cleavage at the 5,6 double bond. CCD4 orthologs may be the CCDs responsible for the production of these volatile apocarotenoids (B.C. Tan, personal communication). CCD8, along with CCD7, is involved in the synthesis of a biologically active compound (See

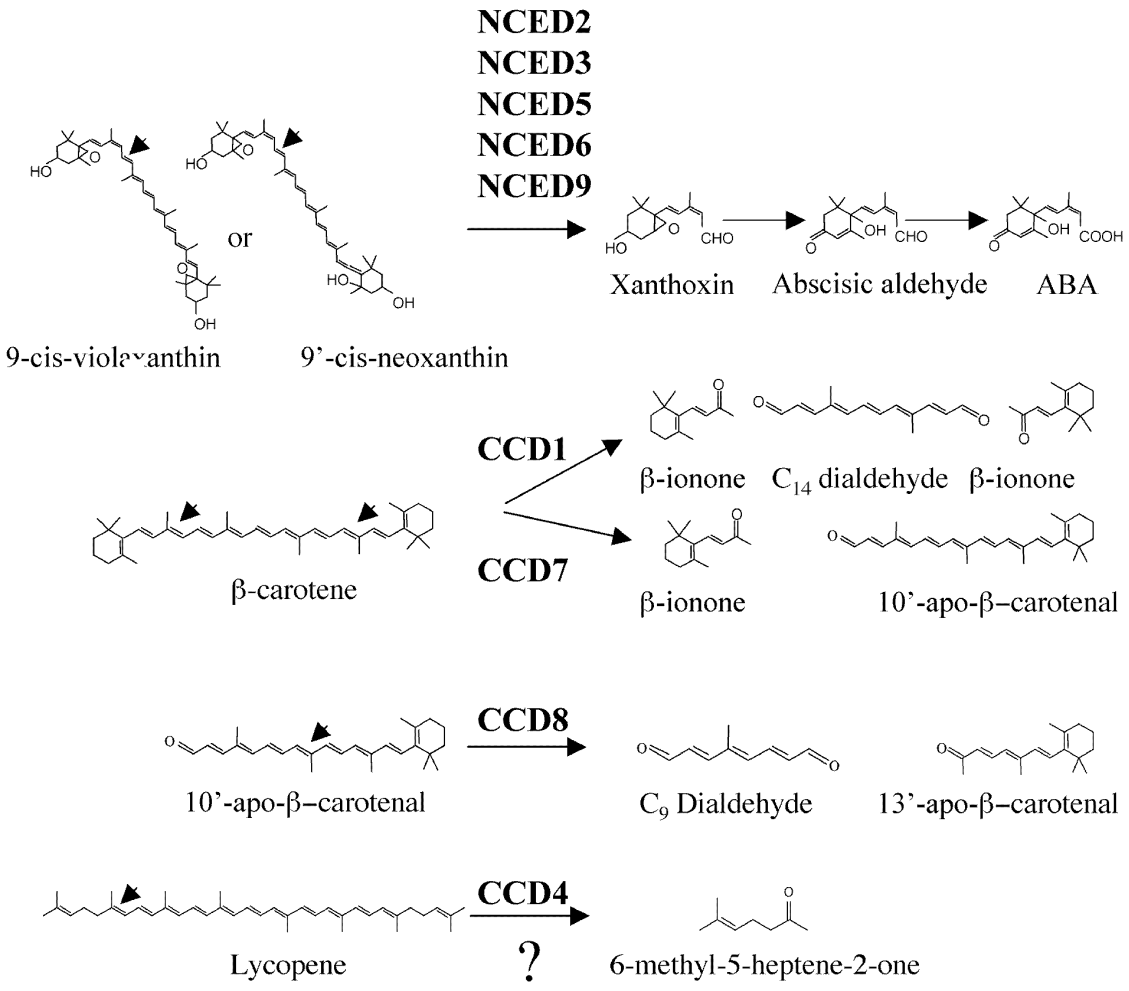

Figure 1-4. Activity of the Arabidopsis CCD family members, showing their divergence in substrate specificity and cleavage site (indicated by small arrows). The NCEDs all cleave 9-cis-epoxycarotenoids at the 11,12 double bond, where as CCD1 and CCD7 cleave a variety of substrates (β-carotene is shown as a representative substrate) at the 9,10 (and/or 9'10') double bond. CCD8 cleaves the C_{27} product of CCD7's activity on β-carotene at the 13,14 double bond. The activity of CCD4 is unknown, however CCD4 has been hypothesized to be the unidentified 5,6 cleaver.

Chapters 3 and 4). The compound has not been identified but CCD8 does show cleavage activity on the C_{27} cleavage product resulting from the activity of CCD7 on β-carotene (Schwartz et al., 2004).

In Summary

Carotenoids are essential plant pigments. They act as both accessory pigments to increase the harvested light used for photosynthesis and as antioxidants to protect the components of the photosystems from oxidative damage (van den Berg, 2000). The catabolism of carotenoids leads not only to regulation of the above mentioned processes but also to the production of secondary metabolites, which may have equally important functions in the plant. These apocarotenoids include the biologically active compounds ABA, retinal and its derivatives, and ß-ionone. Although apocarotenoids are important metabolites in plants, animals and bacteria little is known about the mechanisms involved in their production.

Arabidopsis provides an excellent model system for the study of genes whose products are involved in the production of apocarotenoids. Of the nine carotenoid cleavage dioxygenases identified in Arabidopsis, five have been linked to ABA synthesis (Iuchi et al., 2000; Tan et al., 2003) and one to the production of C_8 apocarotenoids (B.C. Tan, personal communication). The remaining three family members are studied here. The following three chapters discuss the characterization of CCD1, CCD7, and CCD8, respectively. Within each chapter the following topics will be discussed: 1) enzymatic activity of the CCD, either previously determined or elucidated in this study; 2) subcellular, and when appropriate suborganellar, localization of the protein product; 3) analysis of the CCD expression pattern on a whole plant level and as a consequence of

exertion of environmental stimuli such as water stress or day length; and 4) the effect of loss of CCD function on plant development, metabolism, and growth. The subsequent chapter deals with the genetic and molecular interaction of all three CCDs studied and is followed by a discussion on results presented.

CHAPTER 2
CAROTENOID CLEAVAGE DIOXYGENASE 1 (CCD1)

Activity

The Arabidopsis CCD1 cleaves a variety of carotenoid substrates (Schwartz et al., 2001). CCD1 is, however, specific in regard to the site of cleavage, which always occurs at the 9,10 (9',10') double bond irrespective of substrate. This activity was determined both *in vitro* with a recombinant CCD1 enzyme and *in vivo* by way of a heterologous *E. coli* based system (also used for CCD7, see Chapter 3). As an example of its activity, the use of β-carotene as a substrate produces two molecules of the cyclic C_{13} compound, β-ionone, and an acyclic C_{14} dialdehyde, which corresponds to the central portion of the carotenoid molecule (Fig. 2-1). The C_{14} dialdehyde accumulated in the reactions involving CCD1, indicating that it may act as a dimer cleaving both ends simultaneously (Schwartz et al., 2001).

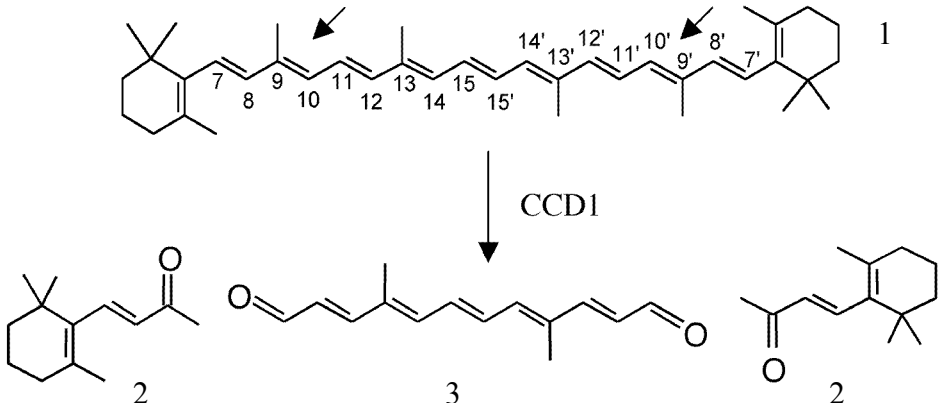

Figure 2-1. CCD1 activity with β-carotene as a substrate. CCD1 cleaves at the 9,10 and 9',10' double bonds of all its substrates. In the case of β-carotene (1), this activity produces two molecules of β-ionone (2) and a C_{14} dialdehyde (3).

Subcellular Localization

The enzymes responsible for carotenoid biosynthesis are located within plastids (Cunningham and Gantt, 1998). Due to their hydrophobic nature carotenoids once synthesized for the most part remain in the plastid. Because CCD1 possesses carotenoid cleavage activity, the possible localization of CCD1 within the plastid was determined. Proteins destined for the plastid typically contain a sequence at their amino terminus called a transit sequence. The protein with its transit sequence attached is a preprotein. Soluble factors within the cytoplasm recognize the transit sequence and chaperone the preprotein to the outer membrane of the plastid. Translocation machinery on both the inner and outer membranes of the plastid inserts the preprotein into the plastid stroma. If the preprotein possesses a cleavable transit peptide, then it is processed into the mature protein by removal of the transit sequence. The mature protein can either remain in the stroma or it can be targeted to the thylakoid, or inner, or outer membranes (Soll and Schleiff, 2004). Although strong conservation in transit sequences does not exist, with the use of computer algorithms a set of general characteristics make it possible to theoretically predict the targeting of a protein into the plastid. CCD1 does not possess a plastid transit sequence, as predicted by the chloroplast prediction program TargetP (v 1.0) (Emanuelsson et al., 2000). In order to experimentally determine the subcellular localization of CCD1, chloroplast import assays were performed following the procedure of Cline et al. (Cline et al., 1993). Briefly, following *in vitro* transcription and translation, the precursor proteins were incubated with isolated pea chloroplasts. After import reactions, intact chloroplasts were treated with the protease, thermolysin. Import into the plastid would protect the proteins from degradation by thermolysin. No import

would allow thermolysin to come into contact with the proteins thus degrading them. The small subunit of ribulose 1,5-bisphosphate carboxylase/oxygenase (ssRubisco), known to be targeted to the chloroplast stroma, was used as a control for import. VP14, the maize NCED, is also chloroplast localized and served as a second comparison. Previously, VP14 was localized to the stroma and, to a lesser extent, associated with the thylakoid membrane (Tan et al., 2001). CCD1 was not imported into the plastid as indicated by its sensitivity to thermolysin treatment (Fig. 2-2). In contrast, both VP14 and ssRubisco were resistant to thermolysin, confirming their import into plastids.

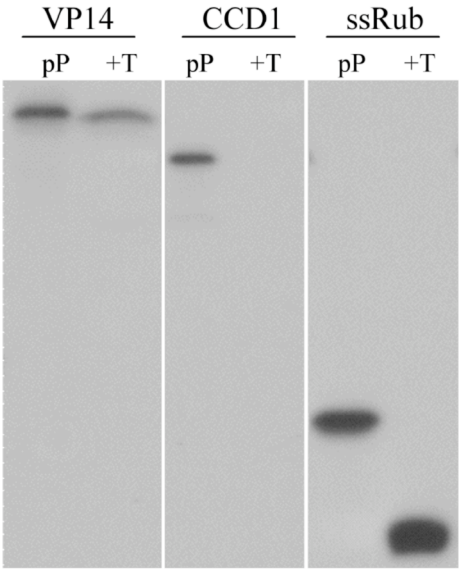

Figure 2-2. Import of *in vitro* transcribed and translated CCD1 precursor protein (pP) into pea chloroplasts compared with ssRubisco (ssRub) and VP14. Following import, chloroplasts were treated with thermolysin (+T).

Expression Analysis

Although transcript expression does not equate with protein accumulation, it does provide information regarding the regulation of the gene in question, whether this be developmental, morphological or as a consequence of external stimuli. An expression

analysis of *CCD1* transcript was performed by a quantitative Real Time RT-PCR method, using Taqman primers and probes. First, the major organs of wild-type Arabidopsis

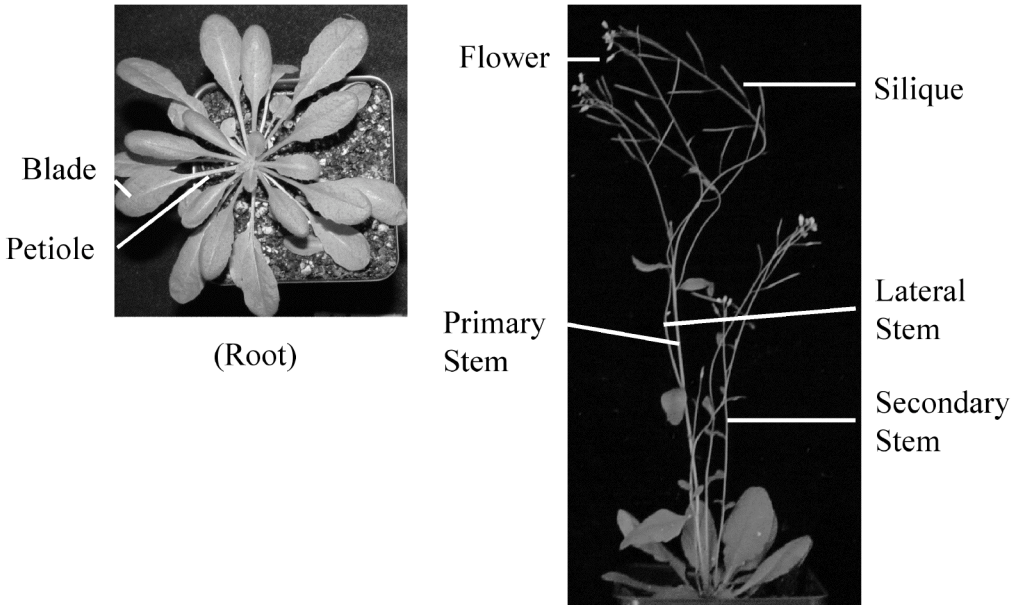

Figure 2-3. Organs of wild-type Arabidopsis used in morphological expression analysis. RNA was extracted from petioles, leaf blades, and roots before bolting. Flowers, siliques, primary and secondary stems were harvested after bolting.

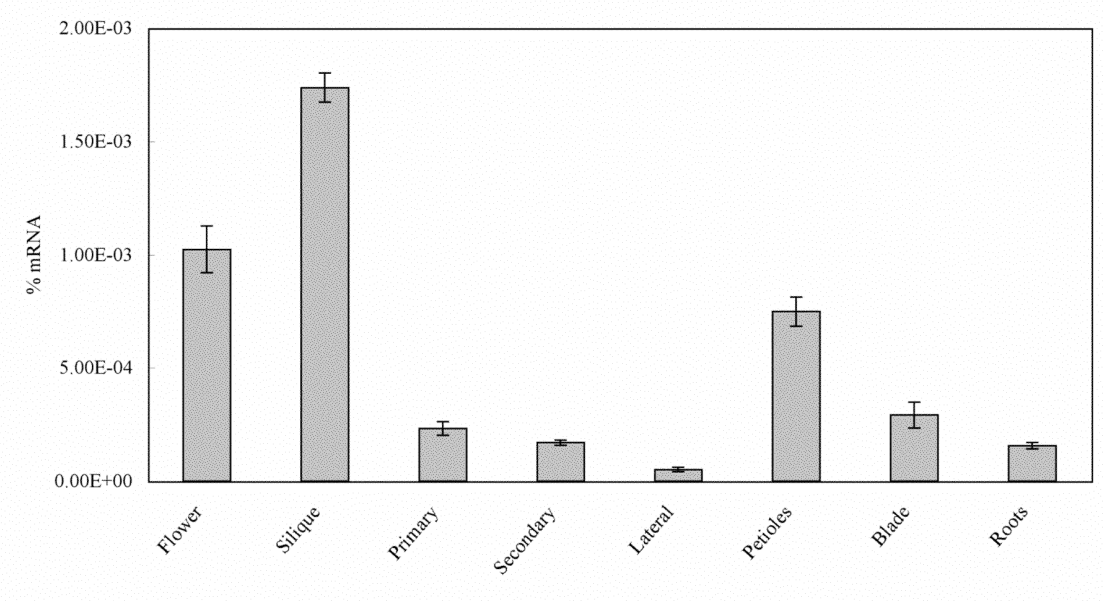

Figure 2-4. Expression pattern of *CCD1* as determined by quantitative Real Time RT-PCR. Data represented as % mRNA after comparison to a standard curve of known quantity. Bars represent standard deviation of the mean.

plants, Columbia ecotype (Col), were dissected and *CCD1* transcript abundance within each was measured. These organs included root, petiole, leaf blade, primary stem, secondary stem, lateral stem, flower, and silique (Fig. 2-3). *CCD1* transcript was present in all organs tested and accumulated to a greater extent in siliques and flowers (Fig. 2-4).

To explore the possible effect of CCD function on ABA-related processes, the effect of drought stress on *CCD1* expression was examined. An increase in expression of all NCEDs was seen following water stress with NCED3 showing the most prominent increase (Tan et al., 2003). The importance of NCED3 in drought stress tolerance was underlined by the observation that transgenic plants lacking NCED3 function were more sensitive to drought stress than wild-type (Iuchi et al., 2001). From activity data CCD1 does not appear to be involved in ABA biosynthesis; however, its expression may be regulated in a drought dependent manner in order to provide more substrates to the NCEDs for ABA production. A water stress was applied to wild-type seedlings by allowing them to lose 15% of their fresh weight. *CCD1* expression did not change significantly as a result of the water stress (Fig. 2-5).

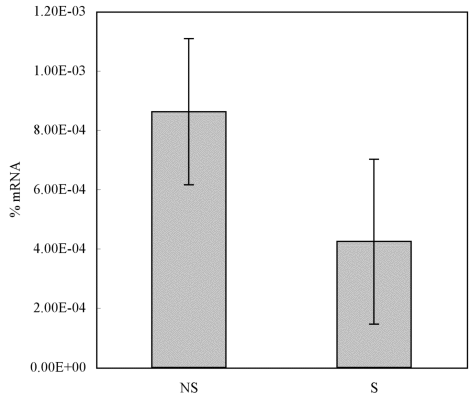

Figure 2-5. Changes in *CCD1* expression due to water stress. *CCD1* expression (± S.E.) found in nonstressed seedlings (NS) and stressed seedlings (S).

Loss-of-Function Mutants

Isolation of Mutant

The function of CCD1 in plant development, metabolism, and growth may be inferred by observations of the effect of its functional loss. A reverse genetics approach was taken to reach this end by isolating insertional mutants from the Wisconsin Knock-out Population (Krysan et al., 1999) and Syngenta's SAIL population (Sessions et al., 2002). See Materials and Methods (Chapter 7, Isolation of loss-of-function mutants) for further discussion on populations and screening process. The insertional mutant from the Wisconsin Knock-out Population was lost during the screening process. However, a mutant was successfully obtained from the SAIL population. The site of insertion of the T-DNA within *CCD1* was verified by first cloning then sequencing the junction. A schematic showing the site of insertion in the 6th intron of *CCD1* is shown in Figure 2-6. As the only *CCD1* loss-of-function mutant isolated this allele was designated *ccd1-1*.

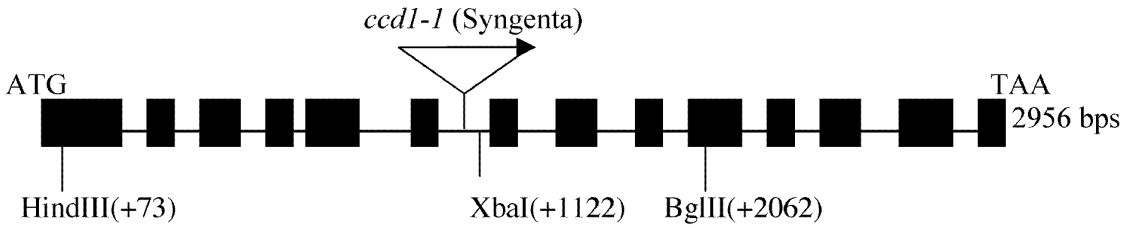

Figure 2-6. Location of T-DNA insert in *CCD1*. Exons are represented by black boxes and introns by intervening lines. The T-DNA insert (inverted triangle) was verified to be within the 6th intron of *CCD1*. Restriction enzymes used for Southern analysis are shown (see below).

Two transformation vectors were constructed for creation of the SAIL population. The pCSA110 vector was used in the transformation event that resulted in *ccd1-1*. The T-DNA present within this vector carries the *BAR* gene for resistance to BASTA, a GUS reporter gene driven by the pollen-specific promoter LAT52, and left and right borders

for transformation with *Agrobacterium tumefaciens* (Fig. 2-7) (McElver et al., 2001). Plants homozygous for the insert were identified by PCR (See Chapter 7, Isolation of loss-of-function mutants). In order to determine T-DNA number within *ccd1-1* plants, DNA from plants homozygous for the T-DNA insertion was extracted and digested for Southern blot analysis using a cloned *BAR* cDNA as the probe (Fig. 2-8). The following restriction enzymes were chosen for digestion of genomic DNA; *Bgl*II, *Xba*I, and *Hind*III. Each of these enzymes cuts within the T-DNA but outside of the *BAR* coding region. Therefore, one band on the Southern indicates a single insertion, two bands indicates two insertions, and so on. Three bands were visible on the autoradiograph in the regions corresponding to lanes containing DNA digested with *Bgl*II or *Hind*III indicating three insertions. Digestion with *Xba*I resulted in one band. This band was of greater intensity than the bands seen in the other lanes possibly as a result of co-migrating pieces of DNA but cannot be interpreted definitively. The Southern analysis indicates the presence of three T-DNA inserts within *ccd1-1* plants.

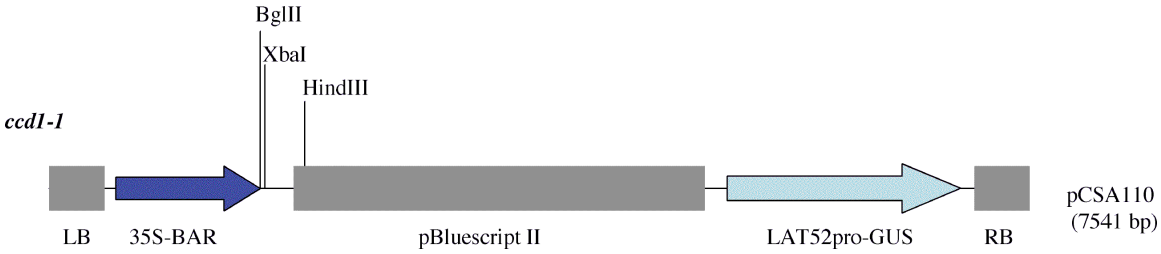

Figure 2-7. Schematic of T-DNA used for transformation to create SAIL population. Locations of restriction enzymes used in Southern analysis of *ccd1-1* are shown.

Morphological Analysis of *ccd1-1*

All mutants from the SAIL population are in the Col ecotype background so all measurements of *ccd1-1* were compared to Col plants. Both Col and *ccd1-1* seeds were planted in soil and grown in short days. Plants were grown until their rosettes

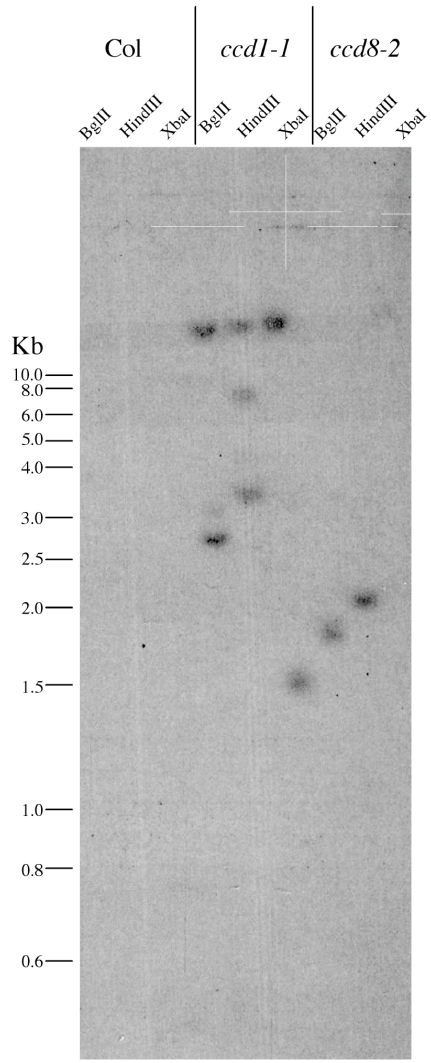

Figure 2-8. Autoradiograph of Southern blot analysis of *ccd1-1* plants. Wild-type (Col) was used as a negative control. Molecular weight markers are shown at left. Enzymes used for digestion are indicated at top. Three T-DNA inserts were found in *ccd1-1* plants. DNA from *ccd8-2* were done on same blot, see Chapter 4.

contained 30-37 leaves at which time measurements of petiole and leaf blade length were taken from the 13th through the 22nd leaf. The *ccd1-1* rosettes prior to bolting were smaller than Col (Fig. 2-9). An average of the 13th through the 22nd leaf (± S.E.) produced data showing *ccd1-1* petioles were significantly shorter than Col (17.80 ±0.35 vs. 19.58 ±0.48, ANOVA P-value = 0.003), whereas leaf blades were not (21.27 ±0.40

Wild-type *ccd1-1*

Figure 2-9. Wild-type (Col) and *ccd1-1* rosettes before bolting. Plants were grown in short days until a leaf number of 30-37 was reached. *ccd1-1* rosettes were smaller than wild-type.

vs. 22.38 ±0.56, ANOVA P-value = 0.136). The significant decrease in petiole length was intriguing as *CCD1* transcript was found to accumulate in petiole tissue (Fig. 2-4). However, upon further review of the measurements both petioles and leaf blades were only smaller than wild-type in the 13th through 16th leaves. The petiole and leaf blade lengths in *ccd1-1* plants increases incrementally from leaf 17 to leaf 22 (Fig. 2-10). Plants were allowed to continue growing in short days until they made the transition to flowering. Infloresence number was counted two weeks following emergence of the primary inflorescence. The inflorescence number of *ccd1-1* plants equaled that observed in wild-type plants (1 ±0.0).

β-ionone Content of *ccd1-1*

CCD1 cleaves several carotenoids at their 9,10 double bonds. This activity was shown with the recombinant enzyme *in vitro* as well as in a heterologous *E. coli* based system (Schwartz et al., 2001). However it has not yet been demonstrated within the plant.

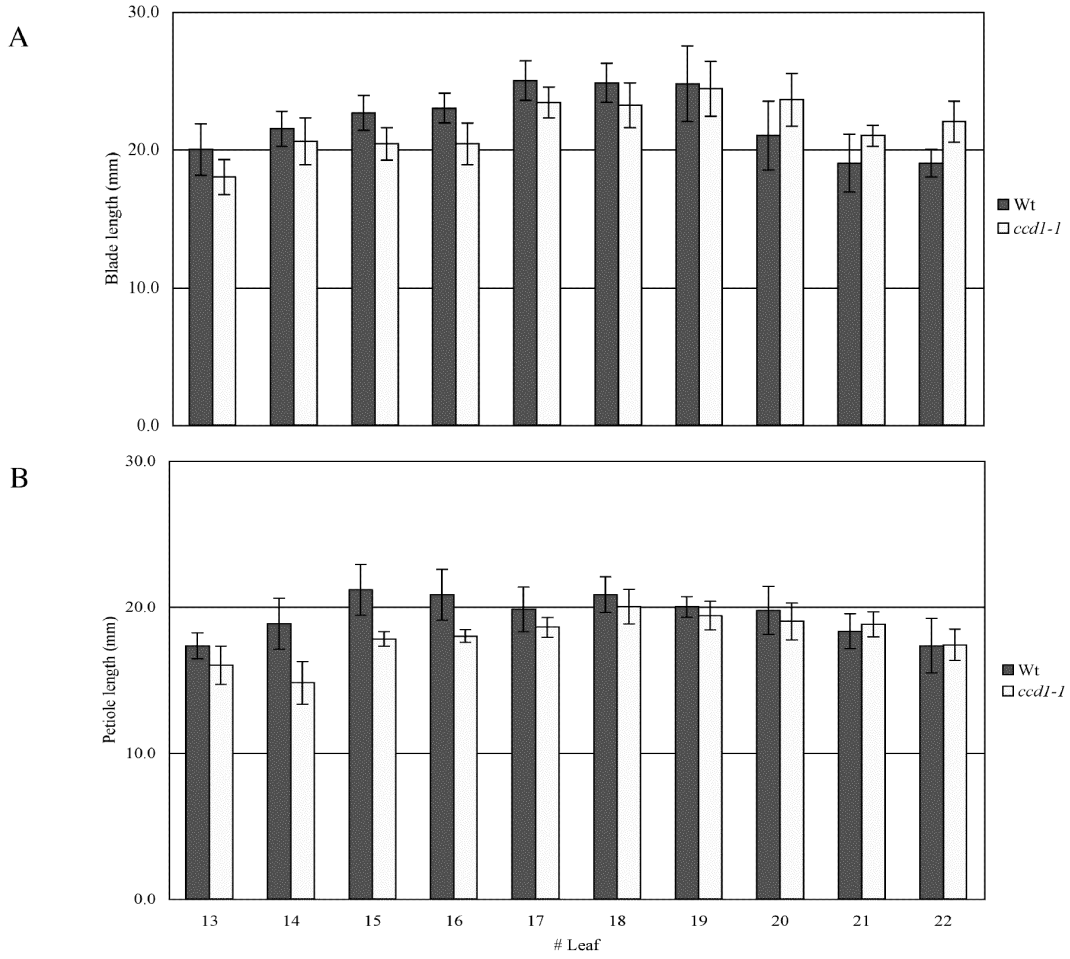

Figure 2-10. Petiole and leaf blade lengths of wild-type (Wt) vs. *ccd1-1* plants. Blade and petiole lengths (± S.E.) of *ccd1-1* were on average smaller than wild-type from leaf number 13 to 16.

The loss-of-function mutant was used to address this issue by determining if loss of a predicted product formed due to CCD1 activity corresponded to a loss in CCD1 function. The product chosen for measurement was β-ionone. CCD1 activity produces two molecules of β-ionone after cleavage of β-carotene at its 9,10 double bonds (Schwartz et al., 2001). β-ionone is a volatile apocarotenoid and as such is thought to be a major constituent of flavor in fruits and vegetables (Winterhalter and Rouseff, 2002). Because of its volatile nature, β-ionone is easily detected by gas chromatography/mass

spectrometry (GC/MS). A method was developed for the extraction and detection of β-ionone from Arabidopsis plants (see Chapter 7, β-ionone Measurements).

β-ionone was found in very small quantities (ng/g tissue) within Arabidopsis rosettes therefore several trials were performed to get an accurate picture of β-ionone production within the plants. Trials consisted of plants grown several months apart but in similar controlled environments. Trial 1 showed a significant decrease in β-ionone within *ccd1-1* plants as compared to Col. Trial 2 only showed a slight, non-significant decrease in β-ionone within *ccd1-1* plants and finally trial 3 showed no change in β-ionone within *ccd1-1* plants (Fig. 2-11). The overall increase seen in Trial 2 plants compared to the other trials may be the result of a fungal gnat infestation within the growth chamber at that period. Increases in β-ionone production have been linked to pathogen infection (Wyatt, 1992). The *ccd1-1* plants in all trials show accumulation of β-ionone indicating the existence of a second CCD responsible for β-ionone production. CCD7 (see Chapter 3) does posses cleavage activity at the 9,10 double bond of β-carotene (Booker et al., 2004; Schwartz et al., 2004). Although, not experimentally tested in the present study, *CCD7* may be regulated such that its levels increase during pathogen infection. Presently, no antibody for CCD1 has been developed therefore the existence of a partially functional CCD1 cannot be overlooked. However, a truncated protein of only 192 amino acids would be possible due to the T-DNA insertion site within *CCD1*.

Determination of Abscisic Acid Content within *ccd1-1* Plants

As a member of the CCD family, CCD1 has sequence homology to VP14, the ABA biosynthetic enzyme from maize. *In vitro*, CCD1 does not posses the same activity as

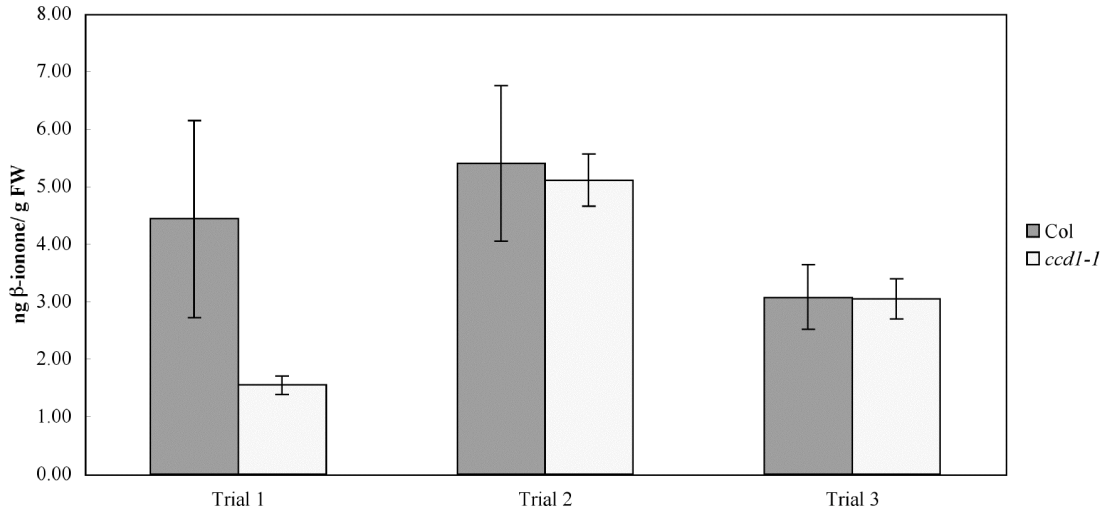

Figure 2-11. β-ionone levels within wild-type (Col) and *ccd1-1* plants measured in three trials. Bars represent standard error of the mean.

VP14 or the Arabidopsis NCEDs. It is unlikely that CCD1 function would have an affect on ABA production. However, the carotenoid substrates of CCD1 are metabolically linked to the carotenoid precursors of ABA in that the carotenoid precursors to ABA are possible CCD1 substrates (Schwartz et al., 2001). For example, a link between the auxin and glucosinolate biosynthetic pathways was discovered after a lesion in the glucosinolate pathway (at CYP83B1) not only resulted in loss of glucosinolates but also plants with auxin overexpression phenotypes (Bak et al., 2001). In a second more unfortunate example, researchers attempting to increase carotenoid content in tomatoes found that their transgenic plants were dwarfed due to a decrease in gibberellin synthesis. Carotenoids and gibberellins share a common precursor in geranyl-geranyl diphosphate such that changes through the carotenoid biosynthetic pathway affected flux through the gibberellin pathway (Fray, 1995). To determine the effect of loss of CCD1 function on ABA biosynthesis, ABA content in *ccd1-1* plants was determined. No alteration in ABA content was seen in the *ccd1-1* plants (Fig. 2-10).

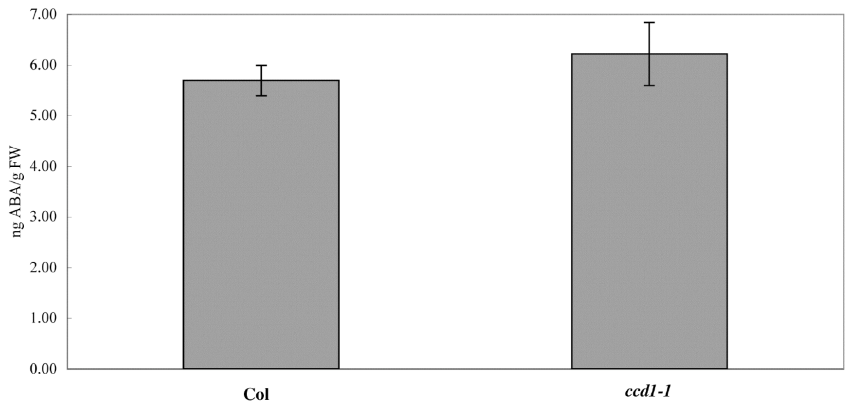

Figure 2-10. ABA content in *ccd1-1* vs wild-type (Col) rosettes. Bars represent standard error of the mean.

In Summary

CCD1 possesses cleavage activity at the 9,10 (9',10') double bond of a variety of carotenoids (Schwartz et al., 2001). Its role in carotenoid catabolism is intriguing because it was not targeted to plastids, the major site of carotenoid accumulation. How CCD1 comes into contact with carotenoids is a further point of study. CCD1 may interact with the plastid outer envelope or may have access to carotenoids only during chloroplast degeneration. The high *CCD1* transcript abundance in flower tissue suggests a biological function because β-ionone, a product of CCD1 cleavage activity on β-carotene, is a known constituent of floral scent. The involvement of CCD1 in plant growth is suggested by the decrease in petiole and leaf blade lengths seen in the loss-of-function mutant. However, a true correlation can only be made after complementation of the petiole phenotype with a wild-type copy of CCD1 is shown. The *ccd1-1*:CCD1OE plants are currently growing. A second on-going experiment concerns the effect of placing CCD1 inside the plastid. This experiment may further our understanding on the localization of CCD1 outside of the plastid as well as provide information regarding the

carotenoid-derived signal found through the analysis of *CCD7* loss-of-function mutants (See Chapter 3 and Chapter 6 for further discussion).

CHAPTER 3
CAROTENOID CLEAVAGE DIOXYGENASE 7 (CCD7)

Activity

Originally designed to identify proteins involved in carotenoid biosynthesis, *E. coli* cells engineered to accumulate certain carotenoid molecules have been utilized as a screen for CCD activity (von Lintig and Vogt, 2000; Kiefer et al., 2001; Redmond et al., 2001; Schwartz et al., 2001). The foundation for these studies is if a protein metabolizes a carotenoid substrate then an observable loss of color would occur upon induction of the protein. The loss of color would be due to metabolism of the accumulating carotenoid and may correspond with an increase in apocarotenoid production. To determine its activity, *CCD7* was expressed in *E. coli* engineered to over-express certain carotenoid biosynthetic genes. The strains utilized in this study accumulated the following carotenoids: phytoene, β-carotene, lycopene, β-carotene, α-carotene and zeaxanthin (Cunningham et al., 1994; Cunningham et al., 1996; Sun et al., 1996). The latter four produced an observable color. However, upon induction of CCD7, color development was diminished, suggesting metabolism of the carotenoid substrates (Fig. 3-1). In order to verify this metabolism, carotenoids were extracted from *E. coli* cultures and analyzed by HPLC (See Chapter 7, Carotenoid/Apocarotenoid Extraction from *E.coli*). CCD7 induction resulted in significant decreases in the carotenoid substrates (Fig. 3-2). The HPLC chromatograms obtained with representative linear (ζ-carotene) and cyclic (β-carotene) carotenoids are shown in Figure 3-3A and B.

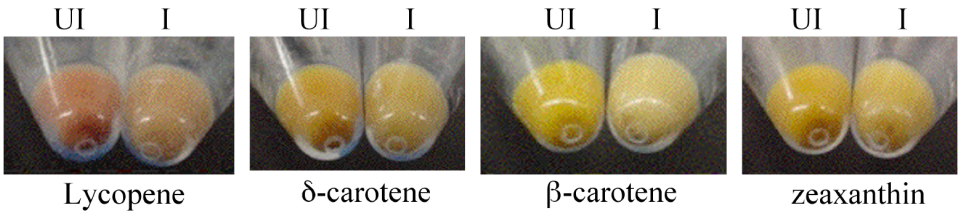

Figure 3-1. *E. coli* lines accumulating lycopene, δ-carotene, β-carotene or zeaxanthin. Lines in which *CCD7* expression was induced (I) was compared to those in which *CCD7* was uninduced (UI).

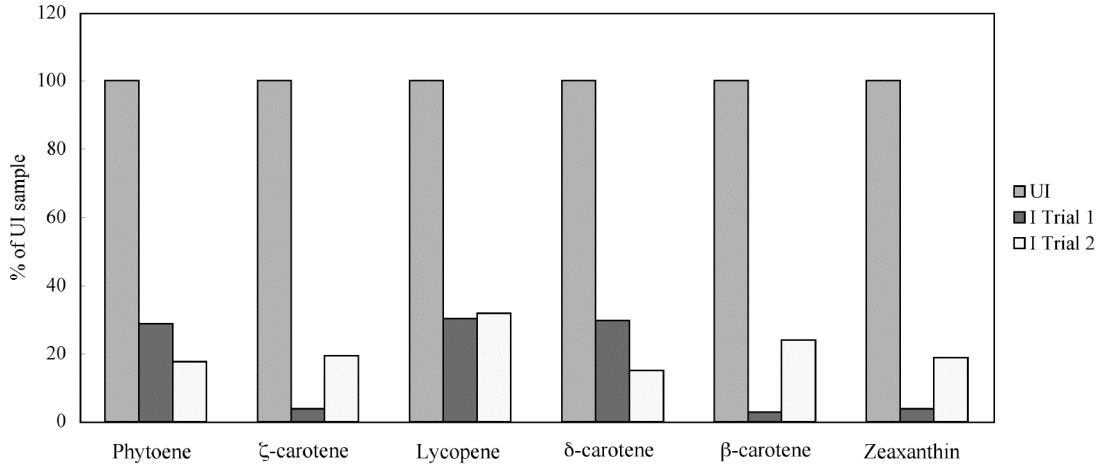

Figure 3-2. Results from HPLC analysis of carotenoid content in each carotenoid accumulating *E. coli* line plus (I) or minus (UI) co-expression of CCD7. Two trials were performed. Data from each trial is expressed as a percentage of uninduced samples.

In order to determine the cleavage site within each carotenoid, GC-MS analysis was used to identify products. Products consistent with cleavage at the 9,10 or 9',10' position were identified in strains that accumulated β-carotene and δ-carotene. Figure 3-3C and D show increases in geranyl acetone (the product of β-carotene cleavage) and β-ionone (the product of δ-carotene cleavage), respectively. Owing to the symmetrical nature of all of the tested carotenoids, these results do not address whether each substrate is cleaved symmetrically or asymmetrically. In each case, the small amounts of geranyl acetone and β-ionone present in the uninduced cultures is likely due to a low level of

expression of *CCD7* prior to induction. These data demonstrate that CCD7 has CCD activity. Schwartz et al. have since reported on the identification of a C_{27} apocarotenoid product resulting from CCD7 activity on ζ-carotene (Schwartz et al., 2004). Here researchers reported optimal activity only when ζ-carotene was used as a substrate.

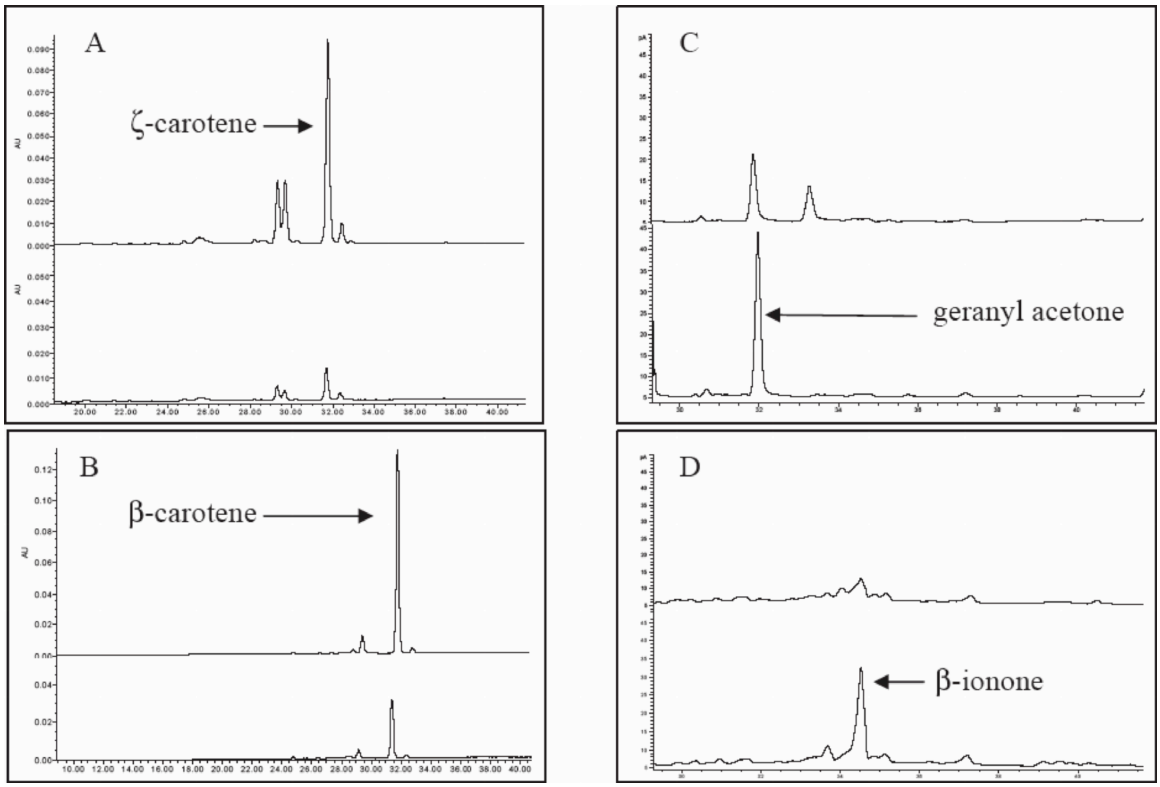

Figure 3-3. Analysis of carotenoid cleavage in *E. coli* expressing CCD7. *E. coli* accumulating either ζ–carotene (A,C) or β–carotene (B,D), either uninduced (top of each panel) or induced (bottom of each panel), were assayed for catabolism of the carotenoid substrate by HPLC (A,B) and production of volatile cleavage products by gas chromatography (C,D). Identities of the indicated volatiles were verified by co-elution with known standards and mass spectrometry.

These studies corroborate the above finding that CCD7 cleaves at the 9,10 double bond and further show that this cleavage is asymmetrical by the identification of the C_{27} apocarotenoid, 10'-apo-ζ-carotene (Fig. 3-4).

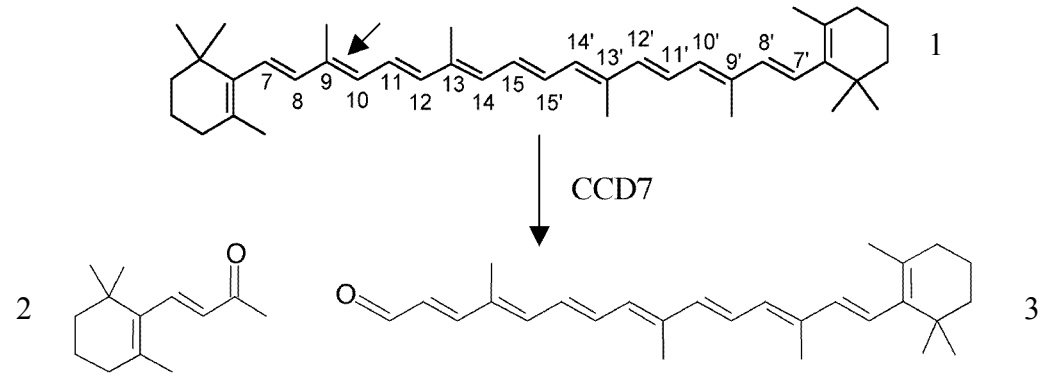

Figure 3-4. Reaction scheme of CCD7 activity on β-carotene (1) as demonstrated by Schwartz et al. (Schwartz et al., 2004). This activity produces β-ionone (2) and 10'-apo-β-carotenal (3).

Subcellular Localization

As with CCD1, the subcellular localization of CCD7 was determined. CCD7 was predicted by TargetP (v 1.0) to be chloroplast localized with a transit peptide of 31 amino acids. Chloroplast import assays were again performed following the procedure of Cline et al. (Cline et al., 1993) using the small subunit of ribulose 1,5-bisphospate carboxylase/oxygenase (ssRubisco) and VP14 as positive controls for import into the stoma and thylakoid.

Following *in vitro* transcription and translation, the CCD7 precursor protein was incubated with isolated pea chloroplasts. After import reactions, intact chloroplasts were either treated with the protease, thermolysin, or fractionated into envelope, stroma, and thylakoid compartments. Results show that CCD7 was resistant to thermolysin treatment, indicating its location inside the chloroplast (Fig. 3-5A). Fractionation of the chloroplast revealed that CCD7 was localized to the stroma (Fig. 3-5B). In addition, the reduced size of the imported mature protein indicated the existence of a cleaved transit peptide. The doublet bands observed may indicate some form of post-import

modification, similar to that observed for several of the Arabidopsis NCED proteins following import (Tan et al., 2003).

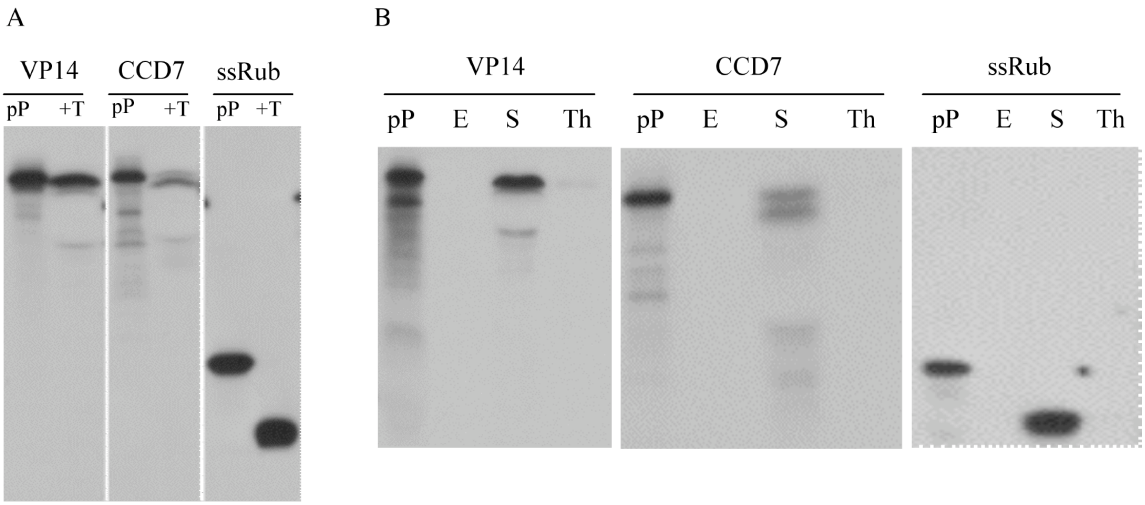

Figure 3-5. Import of *in vitro* transcribed and translated CCD7 precursor protein (pP) into pea chloroplasts compared with ssRubisco (ssRub) and VP14 (A) Following import, chloroplasts were treated with thermolysin (+T). (B) Chloroplasts were further fractionated to determine suborganellar localization to the envelope (E), stroma (S) or thylakiod (Th).

For further verification of plastid localization one additional experiment was performed. Import assays were done using various incubation times. *In vitro* transcribed and translated CCD7 precursor protein was incubated with fresh pea chloroplasts for the following time periods, 0, 1, 2, 4, 8, 15, and 30 minutes. At each time point in order to stop further import, cold import buffer was added to the incubation mixtures, which were then kept in the dark and treated with thermolysin. Figure 3-6 shows that with increasing incubation time CCD7 was more resistant to thermolysin treatment indicating that more of the protein was imported into the chloroplast and therefore protected from degradation by thermolysin.

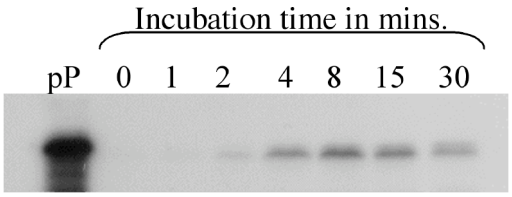

Figure 3-6. Time monitored plastid import assay with CCD7. *In vitro* transcribed and translated CCD7 precursor protein (pP) was incubated with fresh pea chloroplasts for 0, 1, 2, 4, 8, 15, and 30 mins. Following incubation each assay mixture was thermolysin treated.

Expression Analysis

CCD7 transcript abundance was measured by quantitative Realtime PCR using Taqman primers and probes. The tissue used for analysis of expression was dissected in the same way as described in Chapter 2 (Fig. 2-3) for analysis of *CCD1* expression. *CCD7* transcripts were detected throughout the plant. Highest expression was seen in root tissue followed by primary stem tissue and siliques (Fig. 3-7). Even at its highest, *CCD7* trancript abundance was approximately 50-fold lower than the highest *CCD1* expression.

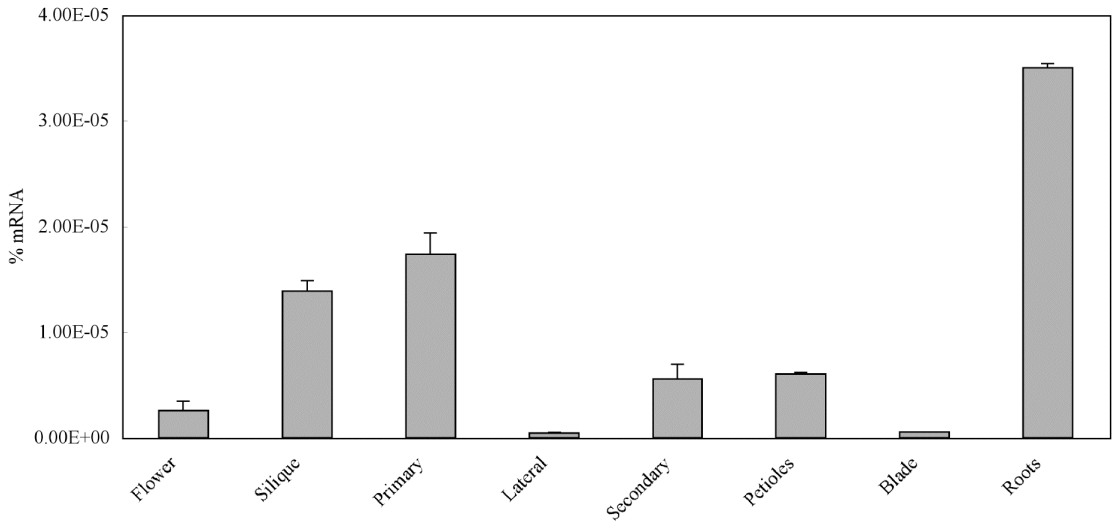

Figure 3-7. Expression analysis of *CCD7* trancript throughout wild-type Arabidopsis plants. *CCD7* expression was observed in all tissue types at very low levels and was found mostly in root issue.

As a consequence of a phenotype seen in the loss-of-function mutants in response to day length (see next section), expression of *CCD7* in whole seedlings grown on short days was compared to seedlings grown on long days. Seedlings were grown for 14 days on a short day light schedule. On the 14th day, a portion of the seedlings was switched to a long day light schedule for five more days. The two groups of seedlings were then compared for any changes in *CCD7* expression. No significant change in *CCD7* expression was apparent (Table 3-1).

Although even less related to VP14 than CCD1 (see Chapter 1), CCD7 does maintain some homology to the ABA biosynthetic proteins. Moreover, CCD7 was shown to have activity on β-carotene, whose content within the plant may affect the content of the epoxycarotenoids, the precursors to ABA. Therefore, CCD7 was also tested for a role in ABA production. As previously stated, all of the Arabidopsis *NCEDs* were shown to have increased expression levels in response to water stress (Tan et al., 2003). In contrast, expression of *CCD7* in seedlings was not altered by a water stress treatment imposed by allowing a 15% loss of fresh weight (Table 3-1).

Table 3-1. *CCD7* transcript abundance in whole seedlings (±SE).

Treatment	% mRNA
Short days	5.57E-06 ±2.38E-06
Long days	4.29E-06 ±1.07E-06
Nonstressed	1.21E-05 ±0.04E-05
Stressed	1.54E-05 ±0.25E-05

ANOVA showed results not to be significant at an P-value=0.05

Loss-of-Function Mutants

Isolation of Mutants

Insertional mutants of *CCD7* were isolated from the Wisconsin Knockout population (Weigel et al., 2000) and the Salk population (Alonso et al., 2003). The alleles were named *max3-10* and *max3-11,* respectively. MAX stands for more axillary branching. Four independent *MAX* loci have been identified and are so named due to the increased number of inflorescences growing out from the axillary meristems of the loss of function mutants (See next section) (Stirnberg et al., 2002; Sorefan et al., 2003; Booker et al., 2004). *MAX3* is *CCD7*. Nine *max3* alleles were identified via an ethyl methane sulfonate (EMS) screen for auxin-associated phenotypes. The two alleles isolated here and reported in Booker et al. sequentially follow the allele designations of the EMS mutants (Booker et al., 2004). The *max3-10* allele is in the Wassilewskija (Ws) background and *max3-11* is in the Columbia (Col) background. The insertion sites are illustrated in Figure 3-8. A primer specific for the left border of the T-DNAs and either a primer specific for a region just upstream of CCD7's start codon (forward) or a primer specific for a region just downstream of its stop codon (reverse) were used to amplify the T-DNA/*CCD7* junction sequence. The junction was cloned then sequenced to verify the T-DNA location within *CCD7*.

In *max3-10*, the left border and forward *CCD7* primer resulted in a product approximately 500 bp in length. The resulting sequence showed that the insert is located within the first exon of *CCD7*. No product was seen using the T-DNA primer and the reverse *CCD7* primer, indicating that the T-DNA and *CCD7* are in the same orientation. In *max3-11*, products were obtained when the left border and either forward or reverse *CCD7* primers were used. Subsequent sequencing placed the inserts within 10 bp of each

other. This suggests the existence of two inserts in reverse orientation to each other. The Salk website used for searching their available insertional mutants illustrates the insert to be in opposite orientation to *CCD7*. The *CCD7* forward and reverse primers used appropriately with the left border primers specific to each T-DNA were used to isolate plants homozygous for the insertion in a segregating population.

The T-DNAs present within each mutant allele are shown in Figure 3-9. The T-DNA within *max3-10* carries a marker for BASTA resistance, four tandemly arranged enhancer elements, and left and right borders for transformation. This vector was constructed for use as an activation tag. However, when present inside the coding region of a gene it is thought to act as a vector for a traditional knock-out approach. The T-DNA within the *max3-11* allele carries a marker for kanamycin resistance as well as

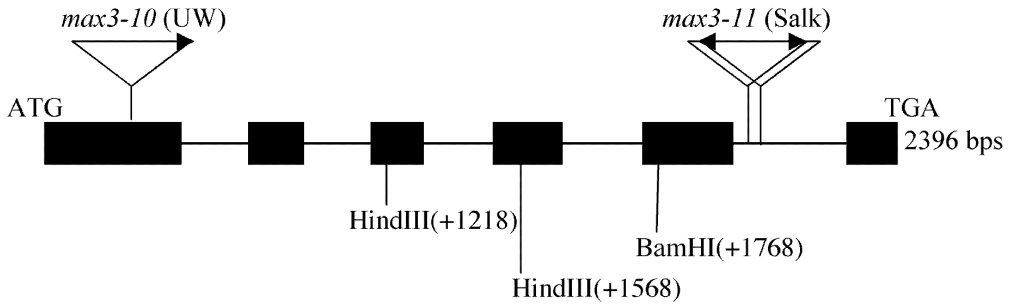

Figure 3-8. Location and orientation of T-DNA inserts in *CCD7*. Exons are represented by black boxes and introns by intervening lines. Sequencing of the T-DNA/gene junction showed *max3-10* contains an insertion (inverted triangle) within the 1st exon and *max3-11* has two insertions within the 5th intron. Arrows indicate orientation of T-DNA in reference to *CCD7* orientation. Location of enzymes used in Southern blot analysis are shown.

components required for transformation. To test for T-DNA number within each mutant the appropriate resistance marker was used as a probe in a Southern blot analysis. The genomic DNA isolated from homozygous *max3-10* plants was digested with *Bgl*II, *Hind*III, or *BamH*I and DNA isolated from homozygous *max3-11* plants was digested

with *Hind*III, *Xba*I, or *BamH*I. The enzymes chosen cut within the T-DNA but outside of the region used as a probe.

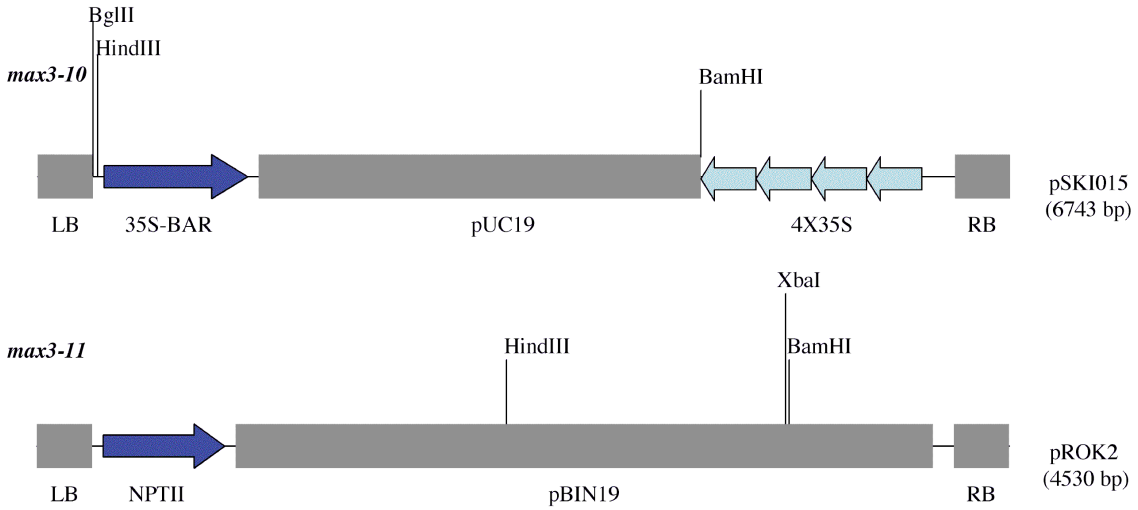

Figure 3-9. Schematic of T-DNA region of vectors used for transformation to create the BASTA population from University of Wisconsin (pSKI015) and the Salk population (pROK2). Location of restriction enzymes used in Southern analysis of *max3-10* and *max3-11* are shown. Resistant markers (shown in blue) were used as probes in Southern analysis.

The wild-type ecotypes were digested and run adjacent to the digestions of each mutant as a negative control. A single band was observed in the Southern of the *max3-10* allele indicating the existence of one T-DNA insert (Fig. 3-10A). Hybridization was weak and was therefore repeated. The second trial gave the same banding pattern but was as weak as the first. Two closely migrating bands were observed for each digestion in the Southern of the *max3-11* allele (Fig.3-10B). As suggested by the PCR results discussed above, Southern blotting indicates that two tandem T-DNA inserts in opposite orientation are present within *max3-11*.

Morphological Analysis of *max3* Plants

The *max3* alleles were grown in soil along with their wild-type counterparts in order to observe any alterations in growth or morphology as a result of the loss of CCD7 function.

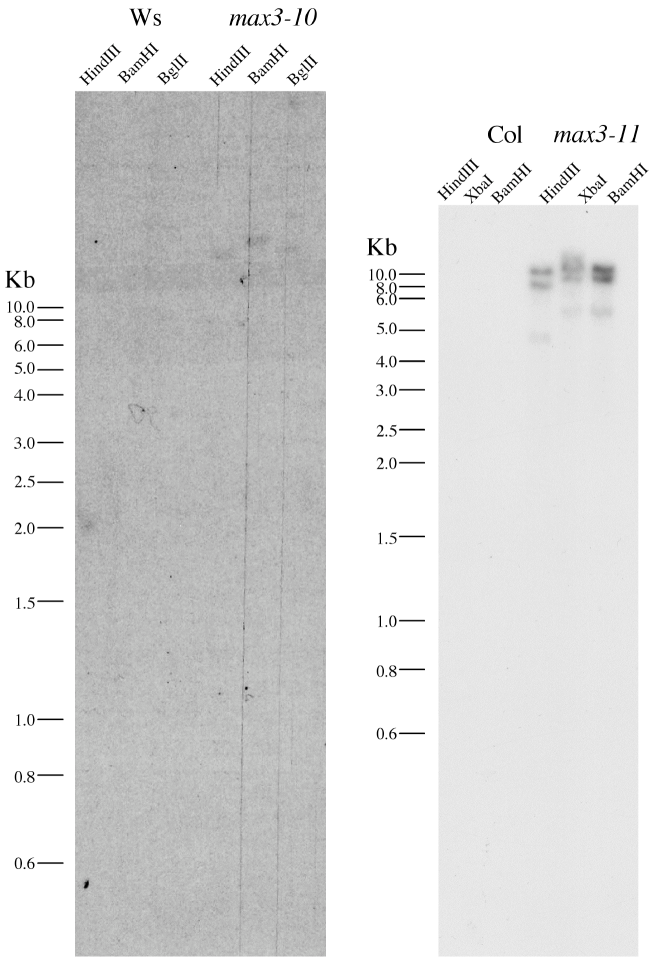

Figure 3-10. Autoradiograph of Southern blot analysis of *max3* plants. Wild-type (Col or Ws) was used as a negative control. Molecular weight markers are shown at left. Enzymes used for digestion are indicated at top.

Both mutant alleles exhibited a branching phenotype and appeared dwarfed in their rosette diameter. These phenotypes were most apparent when grown in short days (Fig. 3-11). To examine the extent of the phenotypes, petiole and leaf blade lengths were recorded from plants grown in short (8h light/16h dark) and long (16h light/8h dark) day conditions. The inflorescence number was also counted. The means and standard errors of all measurements are shown in Table 3-2.

In a short day light schedule, the petioles of *max3-10* and *max3-11* were significantly shorter than wild-type. In a long day light schedule, only the petiole lengths

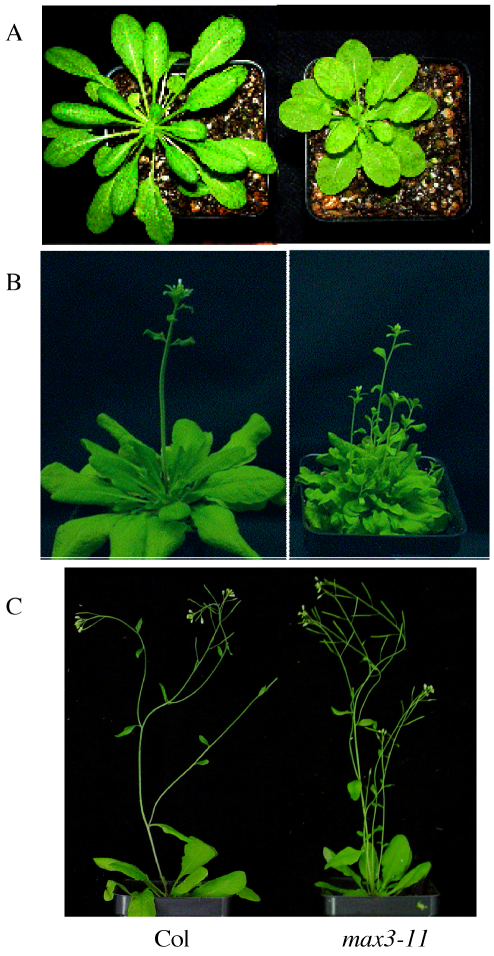

Figure 3-11. Phenotypes of *max3-11* plant compared to wild-type (Col). Plants grown in a short day light schedule (A and B) appeared to have an exaggerated phenotype compared to plants grown in a long day light schedule (C).

of *max3-10* were significantly shorter than wild-type. The *max3-11* leaf blade lengths, although on average shorter, were not significantly different than wild-type in either light regime. The *max3-10* leaf blade lengths were significantly different in short days only, although the difference was an increase in length instead of the expected decrease in length. Inflorescence number was significantly increased in both alleles regardless of light schedule. The increased inflorescence number in the mutants grown in short days was more dramatic than those grown in long days. However, this observation is more likely due to the increase in leaf number at the time of flowering in plants grown in short

days compared to those grown in long days. The increase in leaf number equates to an increase in axillary meristems thus providing a source from which increased shoot growth can occur.

Table 3-2. Petiole and leaf blade lengths and inflorescence number (±SE) taken from *max3* plants grown on short and long days[a,b].

	Petiole (mm)		Leaf Blade (mm)		Inflorescence #	
Day Length	Short	Long	Short	Long	Short	Long
Ws	15.4±1.3	15.5±0.8	13.9±0.9	14.8±1.4	1.1±0.1	1.8±0.4
max3-10	11.3±0.6*	7.7±0.2*	17.8±1.3*	14.7±0.7	7.6±0.8*	4.5±0.2*
Col (5/04)	16.3±1.3	17.4±0.8	14.8±1.4	29.4±1.7	1.0±0.0	1.0±0.2
max3-11 (5/04)	12.0±1.4*	15.9±1.3	11.0±1.6	26.9±2.8	9.3±1.7*	5.1±0.6*
Col (8/04)	———	20.8±1.9	———	18.0±0.9	———	1.8±0.3
max3-9 (8/04)	———	10.7±0.6*	———	17.5±0.3	———	3.7±0.7*
CCD7OE*max3-9* (8/04)	———	15.2±1.2*	———	17.8±0.2	———	1.3±0.2

a. The dates in parentheses next to lines in the Col ecotype are planting dates such that measurements should only be compared between mutant and wild-type planted on same date.
b. The asterisk indicates a significant difference of the mutant allele from its wild-type counterpart (ANOVA, P-value□0.05).

The petiole and leaf blade phenotypes seen in *max3-11* plants were proportionally greater in short days than in long days, thus explaining the enhanced phenotype seen in this growing condition. The *max3-10* plants did not show a greater decrease in either petiole or leaf blade length in short days as compared to long days. This difference may be due to variation in ecotype background. Ws does in fact flower earlier than Col, a trait that has been linked to the natural occurrence of a mutation within the *phyD* coding region (Aukerman et al., 1997). PhyD plays a redundant and less dominant role to phyB in the shade avoidance response, which includes a decrease in time to flowering, increase in elongation growth, and increased apical dominance (Devlin et al., 1999). Although the data in Table 3-2 do not fit into a model suggesting a constitutive shade avoidance response in the *max3-10* allele, the inherent *phyD* mutation may perturb plant growth

such that the petiole and leaf blade lengths between the two mutants cannot be compared. On the other hand, the increase in inflorescence number is consistent between the two mutant alleles.

Complementation of *max3* Phenotype

To confirm that the phenotypes reported above were due to loss of CCD7 function, a wild-type copy of *CCD7* cDNA was cloned from Columbia tissue and put into the vector pDESTOE for *Agrobacterium*-mediated transformation into *max3-9* plants. The *max3-9* line was isolated from the EMS screen (Booker et al., 2004). pDESTOE contains the near-constitutive Figwort Mosaic Virus 35S promoter, the nos terminator, a selectable marker, and elements required for transformation by *Agrobacterium*. The *max3-9:CCD7*OE line used for analysis showed a 3:1 segregation pattern at the T_2 generation indicating the existence of one or multiple linked T-DNA(s). The *max3-9:CCD7*OE plants were taken to homozygosity and were grown along side *max3-9* and wild-type plants in a long day light schedule. Petiole length, leaf blade length, and infloresence number was recorded for all genotypes (Table 3-2). Leaf blade length remained unchanged from wild-type in *max3-9:CCD7*OE plants. Inflorescence number returned to wild-type and petiole length increased from that seen in *max3-9* but did not completely return to wild-type length. To check for high expression of *CCD7* within *max3-9:CCD7*OE plants, *CCD7* transcript abundance was determined within leaves by Real Time RT-PCR. Compared to wild-type, *CCD7* transcript abundance was 30-fold higher in *max3-9:CCD7*OE. Thus, the wild-type copy of *CCD7* complemented the inflorescence phenotype and partially complemented the petiole phenotype seen *max3-9*

plants. Despite the large increase in *CCD7* expression in *max3-9:CCD7*OE no additional phenotypes were evident.

β-ionone Content of *max3-10 and max4-11*

CCD7 possesses activity at the 9,10 double bond of several carotenoid substrates (Booker et al., 2004). This activity was demonstrated to be asymmetrical in nature, such that with β-carotene as a substrate one molecule of β-ionone results (Schwartz et al., 2004). As with *ccd1-1*, mutant alleles of *CCD7* were analyzed for their β-ionone content and compared to their wild-type counterparts in order to assign an *in vivo* activity. Two independent trials were performed (Fig. 3-12B). Trial 1 showed an insignificant decrease and trial 2 showed an insignificant increase in the β-ionone content in *max3-11* compared to wild-type. The changing β-ionone levels observed more than likely reflects a natural variation instead of a change due to loss of CCD7 function.

Interestingly, *max3-10* was markedly increased in β-ionone (Fig. 3-12A). The *max3-10* allele contains a T-DNA within the first exon of *CCD7*. Due to the location of the insert within *CCD7*, the resulting truncated protein produced would contain 461 carboxy terminal amino acids. The wild-type CCD7 contains 618 amino acids, of which the first 56 are predicted to be a cleavable plastid transit sequence. Therefore, it is possible that a functional CCD7 enzyme is produced and led to the increase in β-ionone production seen in *max3-10* rosettes. Schwartz et al. reported that CCD7 retained its activity without its transit sequence (Schwartz et al., 2004). The T- DNA present within *max3-10* is made up of several enhancer elements as it was designed as an activation tag (Weigel et al., 2000). Expression analysis of *CCD7* within *max3-10* rosettes and roots

was compared to expression in Ws. Primers and probe for Real Time RT-PCR lie downstream of the insert location. *CCD7* transcript was greatly increased in the *max3-10*

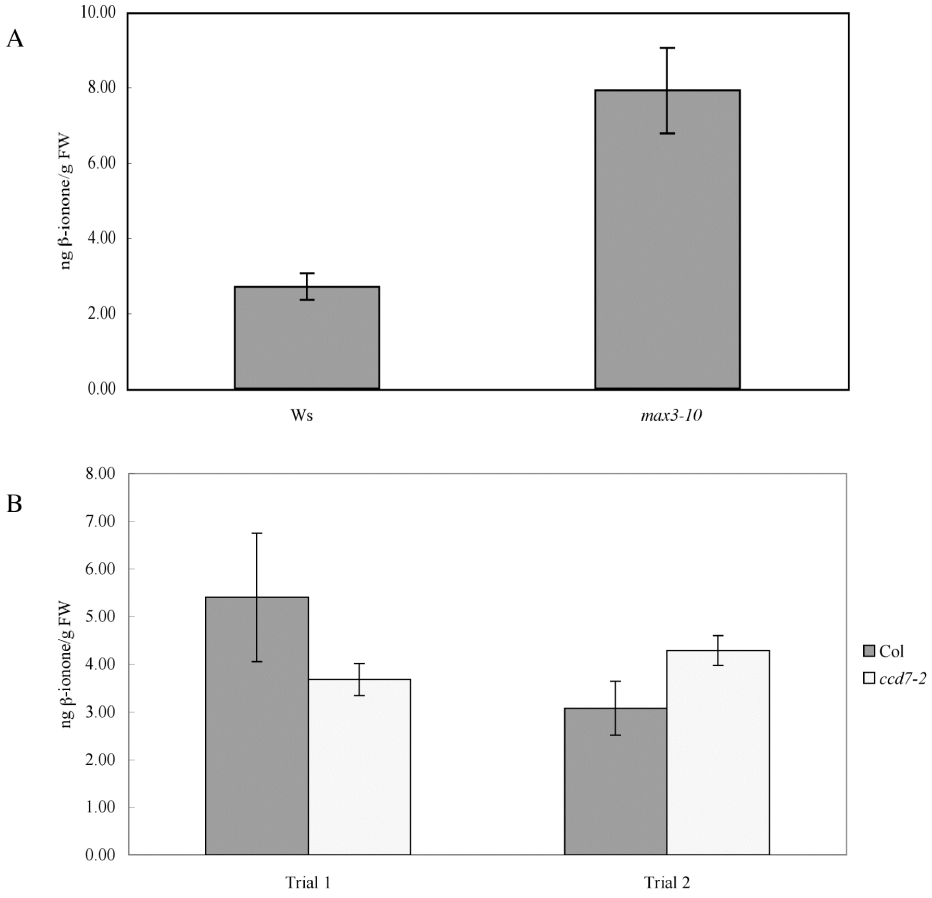

Figure 3-12. β-ionone content in *max3* rosettes. A.) β-ionone content was increased in *max3-10* compared to its wild-type counterpart (Ws) and B.) remained essentially unaltered in *max3-11* compared to its wild-type (Col) counterpart as determined in two independent trials.

tissues (Fig. 3-13). It is feasible that the increased expression of *CCD7* within *max3-10* followed with an increase in accumulation of a functional yet truncated version of CCD7 leading to an increase in β-ionone production. The truncated CCD7 would be without its transit sequence and would therefore not be translocated into the plastid but would contain the five histidines and seven residue sequence conserved among CCDs. Because *max3-10* plants do show the same phenotype as all other *CCD7* mutants, it seems that

localization of CCD7 within the plastid is a requirement for maintenance of a wild-type growth habit.

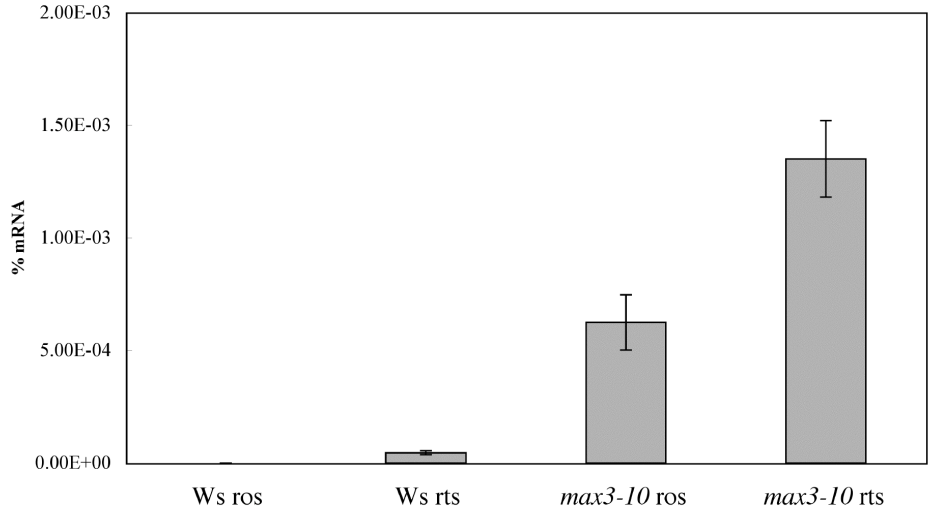

Figure 3-13. *CCD7* expression in *max3-10*. Expression was measured in rosette and root tissue and compared to that seen in the rosette and root tissue of the wild-type background (Ws).

The increase in *max3-10* plants suggests that CCD7 is involved in β-ionone production *in vivo*. Due to the likely mis-localization of CCD7 within *max3-10* plants, it is not known what role CCD7 plays in β-ionone production when inside the plastid. The data from *max3-11* is inconclusive. As mentioned in Chapter 2, the *in vitro* activity of CCD1 also produces β-ionone (Schwartz et al., 2001). The redundancy in activity of CCD1 and CCD7 may explain why β-ionone production was not greatly reduced in *max3-11*. A better genetic background for testing β-ionone production by CCD1 and CCD7 would be the double mutant. The double *ccd1-1max3-11* mutant has been made and is presently being tested for homozygosity. On an additional note, an observable change in β-ionone production due to loss of CCD7 may be improbable due to the very low level of *CCD7* expression (Fig. 3-7). *In vivo* activity of CCD7 may be better

confirmed with an overexpression line, which has been made but not studied for β-ionone content.

Determination of Indole Acetic Acid and Abscisic Acid Content Within *max3-10* Plants

Indole acetic acid (IAA) is an active auxin involved in the maintenance of apical dominance in plants. Auxin originating from the apex of the plant promotes apical dominance (Ward and Leyser, 2004). Lack of auxin perception has been linked to an increased branching pattern in the *axr1* mutants of Arabidopsis (Lincoln et al., 1990; Stirnberg et al., 1999). A direct link between auxin synthesis and branching has been difficult to ascertain likely due to redundancy in the pathway (Cohen et al., 2003). Genes implicated in auxin biosynthesis in plants have been discovered and their overexpression results in apically dominant plants (Zhao et al., 2001; Zhao et al., 2002). To determine if altered auxin content was the cause of the branching phenotype seen in *max3* plants, free IAA was measured in *max3-10* rosettes. IAA levels were not significantly altered in *max3-10* rosettes. (Fig. 3-14).

CCD7 was also tested for its possible involvement in ABA production by ascertaining ABA content with the *max3-10* mutant and comparing it to wild-type. While ABA has been implicated in bud inhibition (Chatfield et al., 2000), none of the NCED loss-of-function mutants display a shoot branching phenotype (B.C. Tan and W.T. Deng, personal communication). ABA levels were essentially equal to wild-type (Fig. 3-14). Therefore, CCD7 does not play a role in ABA synthesis.

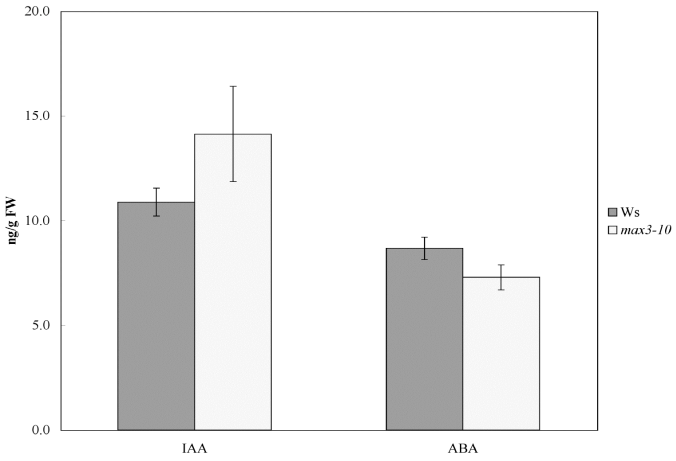

Figure 3-14. IAA and ABA content within *max3-10* rosettes compared to wild-type (Ws).

In Summary

CCD7 is a carotenoid cleavage dioxygenase with activity at the 9,10 double bond of a variety of carotenoid substrates (Booker et al., 2004). CCD7 is a soluble plastid localized protein that accumulates in the stroma. Its transcript was found highest in the root tissue of adult plants but was low in expression compared to other CCDs studied. Expression was not altered by day length or by imposition of a water stress. Plants without a functional CCD7 lack the ability to maintain apical dominance and as a result are bushy in appearance. Rosette size is also affected by the presence of CCD7 function. This functionality is dependent on localization of the protein product within the plastid. From these results, it seems CCD7 is involved in the production an apocarotenoid compound that is required for the normal inhibition of shoot growth from axillary meristems. It is not known whether the change in rosette size is a direct result of loss of CCD7 function or if it is an indirect result of early growth from typically dormant meristems.

CHAPTER 4
CAROTENOID CLEAVAGE DIOXYGENASE 8 (CCD8)

Activity

Using the same heterologous *E. coli* system used to determine the activity of CCD1 and CCD7, Schwartz et al. determined CCD8 cleavage activity (Schwartz et al., 2004). CCD8 was shown to cleave at the 13,14 double bond of the apocarotenoid produced by the activity of CCD7 on β-carotene. When *CCD8* was expressed alone in the β-carotene accumulating line no apocarotenoid products were observed. CCD8 activity was dependent on the presence of CCD7. Only upon induction of both CCD7 and CCD8 in the same β-carotene accumulating *E. coli* strain did the accumulation of 13'-apo-β-carotene and a C_{18} dialdehyde product result (Fig. 4-1). These products were thought to be derived from the cleavage of 10'-apo-β-carotene (the product of CCD7's activity on β-carotene) at its 13,14 double bond. Therefore, a biochemical pathway can be drawn in which β-carotene is metabolized to 13'-apo-β-carotene and the C_9 dialdehyde product in a two-step reaction involving both CCD7 and CCD8 (Schwartz et al., 2004).

Subcellular Localization

Localization of CCD8 within plastids was determined following the same procedures as with CCD1 (Chapter 2) and CCD7 (Chapter 3). The chloroplast prediction program TargetP (v 1.0) (Emanuelsson et al., 2000) predicts CCD8 to be chloroplast localized and assigns a transit peptide of 56 amino acids. Chloroplast import assays with the use of the protease thermolysin (Cline et al., 1993) verified its localization to the

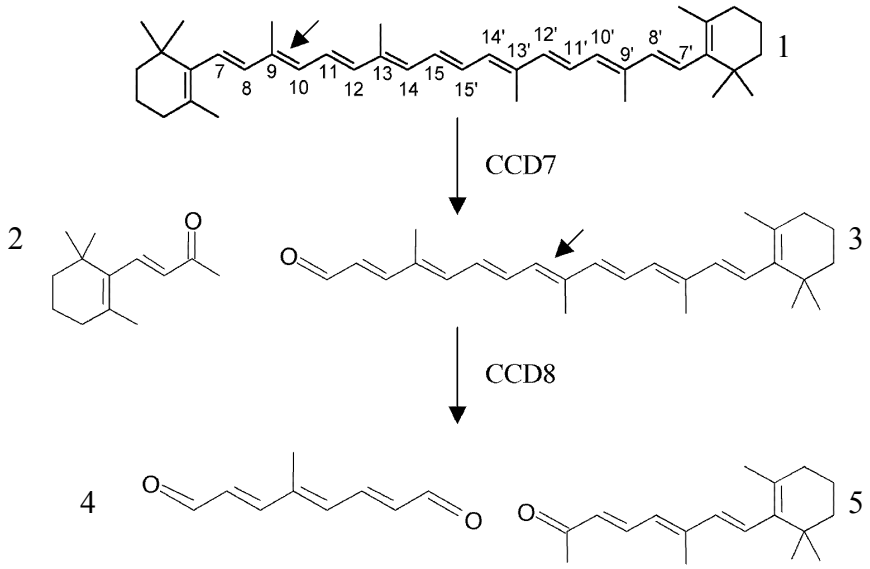

Figure 4-1. Proposed activity of CCD8. CCD8 may act on the 13,14 double bond of 10'-apo-β-carotenal (3), one product resulting from CCD7's activity on β-carotene (1), the other product being β-ionone (2), to produce a C_9 dialdehyde (4) and 13'-apo-β-carotene (5).

chloroplast (Fig. 4-2A). Fractionation of the chloroplast revealed that CCD8 was localized to the stroma (Fig. 4-2B). In addition, the reduced size of the imported mature protein indicated the existence of a cleaved transit peptide.

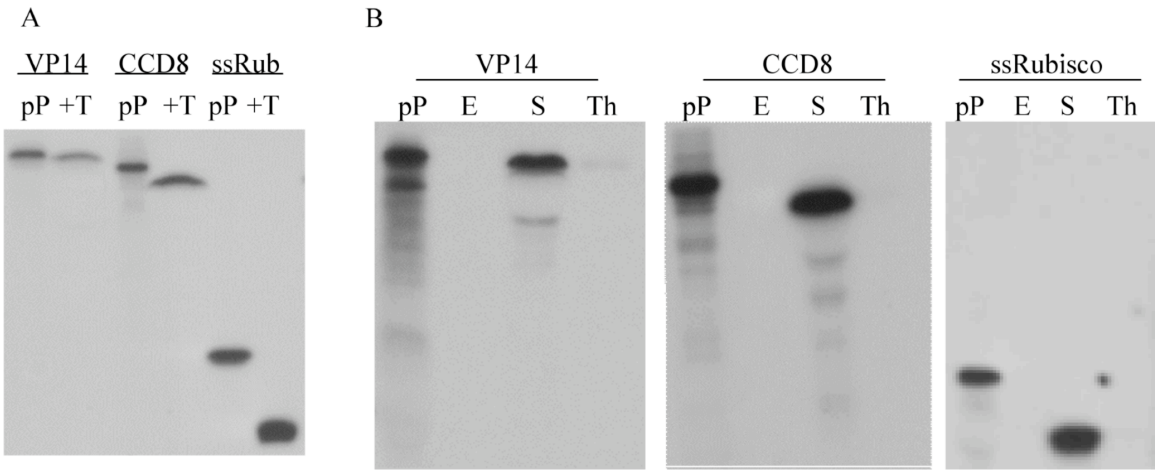

Figure 4-2. Import of *in vitro* transcribed and translated CCD8 precursor protein (pP) into pea chloroplasts compared with ssRubisco (ssRub) and VP14. (A) Following import, chloroplasts were treated with thermolysin (+T). (B) Chloroplasts were fractionated to determine suborganellar localization to the envelope (E), stroma (S) or thylakoid (Th).

Incubation of *in vitro* transcribed and translated CCD8 precursor proteins with fresh pea chloroplasts for 0, 1, 2, 4, 8, 15, and 30 minutes showed that with increasing incubation time CCD8 was more resistant to thermolysin treatment (Fig. 4-3). It could then be concluded that, as with CCD7, CCD8 was imported into the chloroplast stroma.

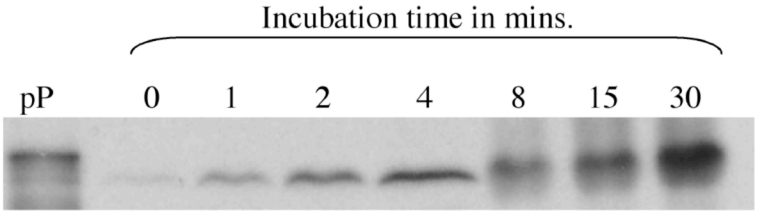

Figure 4-3. Time monitored plastid import assay with CCD8. *In vitro* transcribed and translated CCD8 precursor protein (pP) was incubated with fresh pea chloroplasts for 0, 1, 2, 4, 8, 15, and 30m. Following incubation each assay mixture was thermolysin treated.

Expression Analysis

As with *CCD1* and *CCD7* (Chapters 2 and 3, respectively), *CCD8* transcript abundance was measured by quantitative Real Time RT-PCR using Taqman primers and probes. RNA was extracted from tissue dissected from wild-type adult plants in the same way as described in Chapter 2 (Fig. 2-3). Figure 4-4 shows transcript abundance as a percentage of mRNA calculated by comparison to a standard curve. *CCD8* transcripts were detected in all tissues tested albeit at low levels. Interestingly, highest expression was seen in root tissue prior to bolting (Fig. 4-4A). Previously, it was shown that wild-type roots grafted onto *CCD8* mutant shoots rescued the phenotype associated with loss of CCD8 function (Sorefan et al., 2003). Thus, the increased expression seen in roots relative to other tissue was intriguing. We therefore compared root expression before and after emergence of the primary inflorescence, and after emergence of secondary inflorescences (Fig. 4-4B). Transcript abundance in root tissue decreased by an average

of 65% after the emergence of primary and secondary inflorescences. In contrast, the low level of transcript in leaf blade was not altered after axillary shoot emergence.

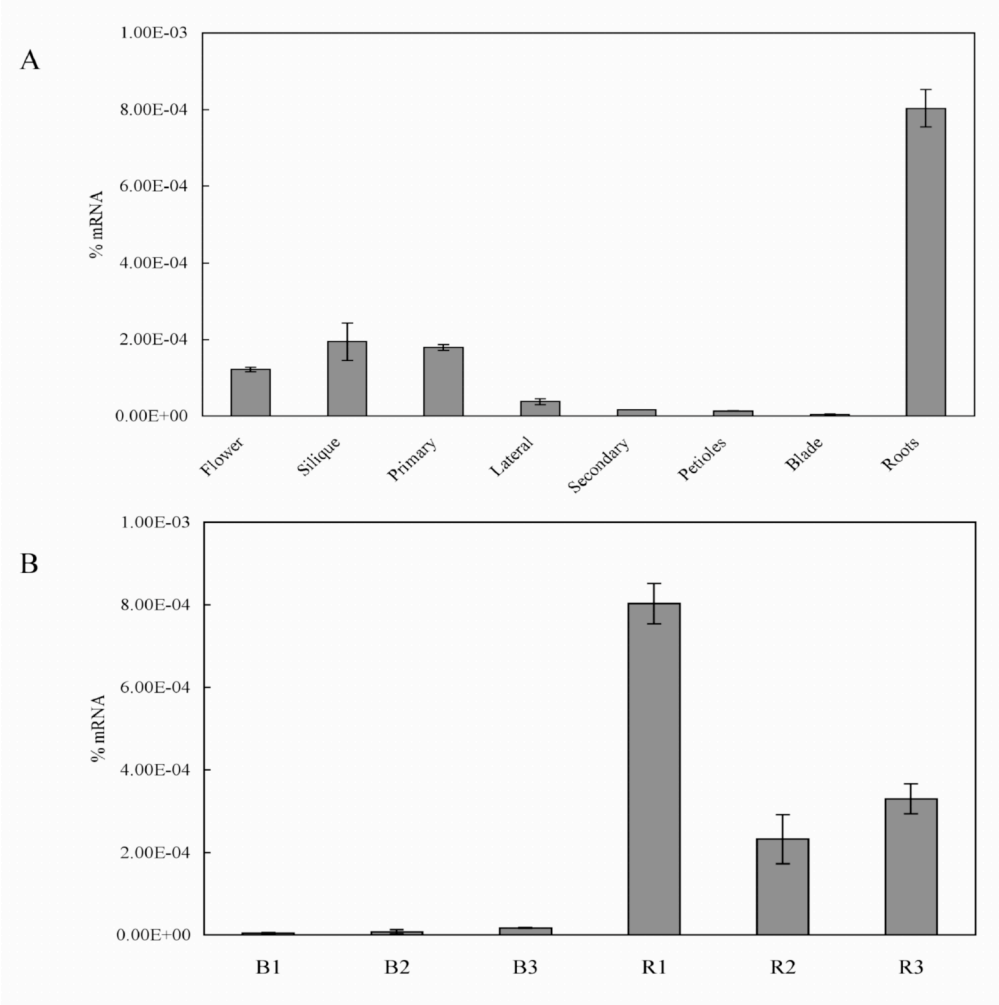

Figure 4-4. Expression pattern of *CCD8* as determined by Real Time PCR. A.) RNA was extracted from petioles, leaf blades, and roots before bolting. B.) Comparison of expression in leaf blade and root tissue at three developmental time points, B1, leaf blade before bolting; B2, leaf blade after emergence of primary inflorescence; B3, leaf blade after emergence of secondary inflorescences; R1, root before bolting; R2, root after emergence of primary inflorescence; R3, root after emergence of secondary inflorescences.

CCD8 loss-of-function mutants showed a similarly enhanced phenotype as *CCD7* mutants did in short day growth conditions (See next section). A day length effect on *CCD8* expression was also tested. Expression of *CCD8* in whole seedlings grown on

short days was compared to seedlings grown on long days following the same procedure as in Chapter 3. In unison with *CCD7*, no significant change in *CCD8* expression was apparent (Table 4-1). Therefore, the enhanced mutant phenotype seen in short days when compared to long days does not appear to be a consequence of *CCD8* transcription and/or RNA turnover.

Following suit with the relationship of CCD1 and CCD7 on ABA production, CCD8 was tested for its role in ABA biosynthesis by determining the effect of water stress on its expression. As with *CCD1* and *CCD7*, expression of *CCD8* in seedlings was not altered by a water stress treatment imposed by allowing a 15% loss of fresh weight (Table 4-1).

Table 4-1. *CCD8* transcript abundance in whole seedlings (±SE).

Treatment	% mRNA
Short days	2.13E-05 ±0.23E-05
Long days	2.74E-05 ±0.70E-05
Nonstressed	4.04E-05 ±1.04E-05
Stressed	3.35E-05 ±1.09E-05

ANOVA showed results not to be significant at an α=0.05

Loss-of-Function Mutants

Isolation of Mutants

Two independent loss-of-function mutants for *CCD8* were isolated from the Wisconsin Knockout facility (Krysan et al., 1999) and the SAIL population (Sessions et al., 2002). Because mutants of *CCD8* (*max4-1* through *max4-4*) have previously been isolated (Sorefan et al., 2003), the mutants discussed here will follow the established nomenclature for mutant designation, i.e. the mutant isolated from the Wisconsin Knock-

out facility was named *max4-5* and the mutant obtained from Syngenta's SAIL population was named *max4-6*.

To verify the location of the T-DNA inserts, the junction of the T-DNA and *CCD8* was amplified using a *CCD8* forward or reverse specific primer and a primer specific for the left border of the T-DNA. DNA from *max4-5* produced a product approximately 800 bp in size using the *CCD8* reverse primer and left border primer. The amplified DNA was cloned and subsequent sequencing placed the insert within the fourth exon of *CCD8* (Fig. 4-5). No product was obtained using the *CCD8* forward primer indicating that the T-DNA was in reverse orientation relative to *CCD8*.

A product approximately 3.2 kbp in size was amplified from *max4-6* DNA when using the *CCD8* forward primer and left border primer. Sequencing placed the insertion in the fifth exon of *CCD8* (Fig. 4-5). A product of approximately 500 bp was obtained using a *CCD8* reverse primer and left border primer. This fragment was also sequenced and placed the insert 17 bp downstream of the original placement. Positive amplification with both *CCD8* forward and reverse primers indicates the presence of two tandem T-DNAs in opposite orientation. For both alleles, the *CCD8* forward or reverse primer used with the left border primer specific to each T-DNA was used to isolate a plant homozygous for the insertion in a segregating population.

The T-DNAs present within each mutant allele are shown in Figure 4-6. The *max4-5* allele was isolated from the University of Wisconsin's Alpha population. The transformation vector used to create these lines is a derivative of pD991 and is called pD991-AP3. The T-DNA within this vector contains the left and right border sequences

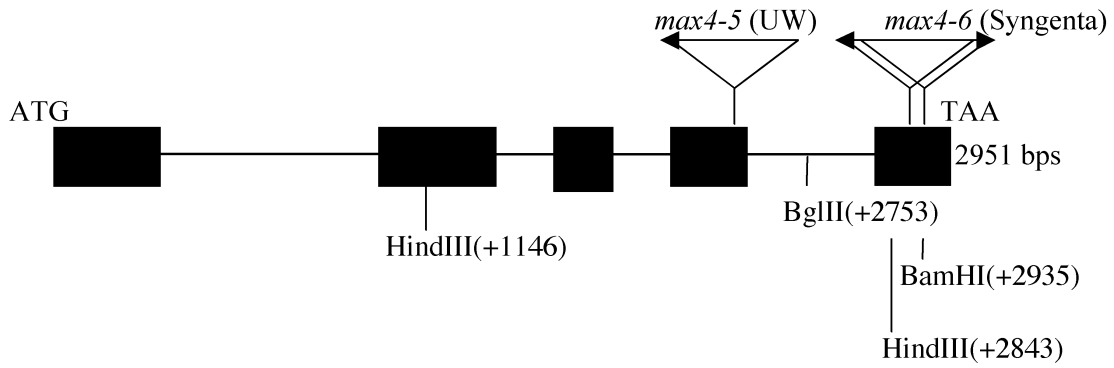

Figure 4-5. Positions of T-DNA insertions within *CCD8*. Black boxes are exons, intervening lines are introns, and inverted triangles represent T-DNA inserts. Sequencing of the T-DNA/gene junction showed *max4-5* contains an insertion (inverted triangle) within the 4th exon and *max3-11* has two insertions within the 5th exon. Locations of enzymes used in Southern blot analysis are shown. Arrows indicate orientation of T-DNA in reference to *CCD8* orientation.

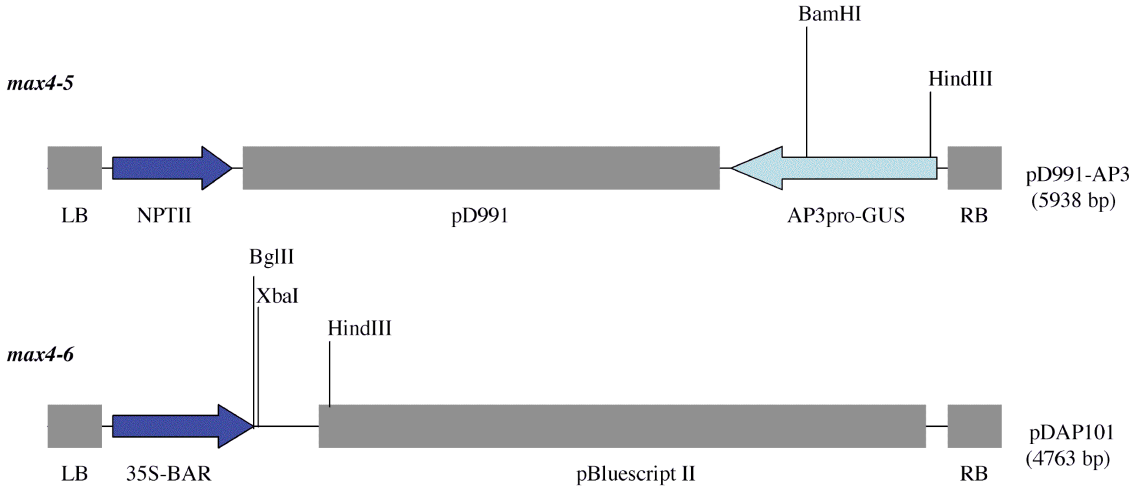

Figure 4-6. Schematic of T-DNA region of vectors used for transformation to create the Alpha population from University of Wisconsin (pD991-AP3) and the Syngenta population (pDAP101). Location of restriction enzymes used in Southern analysis of *max4-5* and *max4-6* are shown.

for transformation with *Agrobacterium*, the *nptII* gene for resistance to kanamycin and a GUS gene driven by the AP3 promoter (Krysan et al., 1999). The *max4-6* allele was obtained from the SAIL population. The vector used for transformation in this population is pDAP101. The T-DNA within this vector contains only the border sequences and a 35S driven BAR gene for resistance to BASTA. To test for T-DNA

number within each mutant the appropriate resistance marker was used as a probe in a Southern blot analysis. The genomic DNA isolated from *max4-5* plants was digested with *Bgl*II, *Hind*III, or *BamH*I and DNA isolated from *max4-6* was digested with *Bgl*II, *Hind*III, or *Xba*I. The enzymes chosen cut within the T-DNA but outside of the region used as a probe with one exception, *Bgl*II does not cut within the T-DNA of pD991-AP3.

The wild-type ecotypes were digested and run adjacent to the digestions of each mutant as a negative control. A single band was observed in the Southern of the *max4-6* allele indicating the existence of one T-DNA insert (Fig. 4-7). However the PCR results discussed above argue for two T-DNA inserts. Rearrangements and partial insertions are common occurrences in *Agrobacterium* mediated transformation events (Meza et al., 2002; Windels et al., 2003). It is possible that a partial insertion occurred where enough of the left border sequence was inserted to allow for amplification by PCR of a junction sequence. Two bands were observed in the Southern of the *max4-5* allele when digested with *BamH*I or *Bgl*II, indicating two T-DNAs within *max4-5*. Only one band was present in the *Hind*III digestion, however this band was of a greater intensity than the other bands, likely due to the presence of two bands of equal size (Fig. 4-7). It is possible that the second T-DNA is not within *CCD8* but must be within a short distance from it as selection of a segregating population on kanamycin resulted in a 3:1 segregation of kanamycin resistant to sensitive seedlings (74 seedlings total, 57 kanamycin resistant: 17 kanamycin sensitive).

Despite the 3' location of the T-DNAs within each mutant allele, activity of the truncated forms of these proteins is unlikely because the insertions disrupt *CCD8* upstream of the codon for at least one of five histidine residues conserved in all

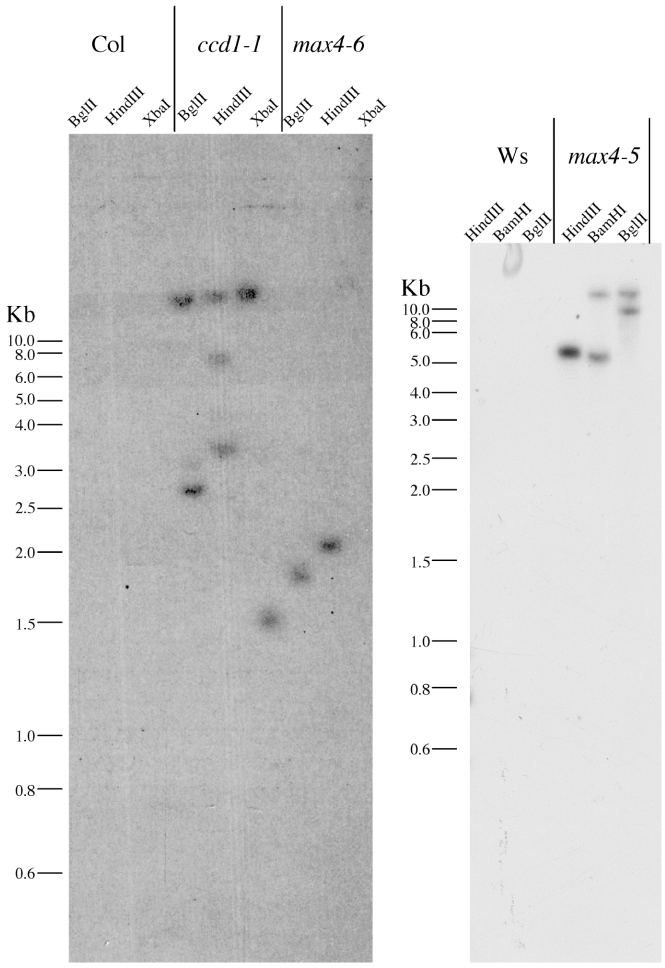

Figure 4-7. Autoradiograph of Southern blot analysis of *max4* plants. Wild-type (Col or Ws) was used as a negative control. Molecular weight markers are shown at left. Enzymes used for digestion are indicated at top.

carotenoid cleavage dioxygenases. These five conserved histidines are thought to coordinate a non-heme iron. Dioxygenase activity of VP14 (Schwartz et al., 1997) and the Drosophila 15,15' dioxygenase (von Lintig and Vogt, 2000) has been shown to be dependent on the presence of iron. If a truncated version of CCD8 resulted in *max4-5* plants it would be without two of the five conserved histidines and a highly conserved seven residue sequence found in plant and animal carotenoid cleavage dioxygenases. A truncated CCD8 in *max4-6* plants would be without one of the histidine residues,

highlighting the importance of each histidine in the fully functional protein as each mutant allele confers the same phenotype (see next section).

Morphological Analysis of *max4* Plants

Seeds homozygous for T-DNA insertions were planted with their wild-types in soil. The plants of both *CCD8* loss-of-function alleles were highly branched. The axillary buds, which are typically delayed in growth in wild-type plants, grew out to produce leaves and inflorescences, a phenotype almost identical to the *CCD7* loss-of-function mutants. Again, the phenotype was most obvious when grown on short days (Fig. 4-8). Petiole length, leaf blade length and inflorescence number were recorded in short and long day growth conditions. Like the *max3* mutants, the *max4-5* and *max4-6* plants had smaller rosette diameters due to a decrease in the lengths of petioles compared to wild-type plants (Table 4-2). The decrease in petiole length was significant in both growing conditions. Unlike *max3*, the leaf blade lengths were decreased in both *max4-5* and *max4-6* grown on long days and *max4-6* grown on short days. Leaf blade lengths of *max4-5* grown on short days were actually longer than wild-type, an observation consistent with the *max3-10* mutant. Both *max4-5* and *max3-10* are in the Ws background. The increase in leaf blade length instead of the decrease seen in the *max4-6* and *max3-11* mutants may be due to ecotype variation. Inflorescence number was increased in both *max4* alleles under short and long day conditions. In long days, the increase was similar to that seen in the *max3* alleles but was stronger than *max3* in short days.

Complementation of *max4* Phenotype

The pDESTOE transformation vector was used to introduce a wild-type copy of the *CCD8* cDNA under the control of the constitutive Figwort Mosaic Virus 35S promoter

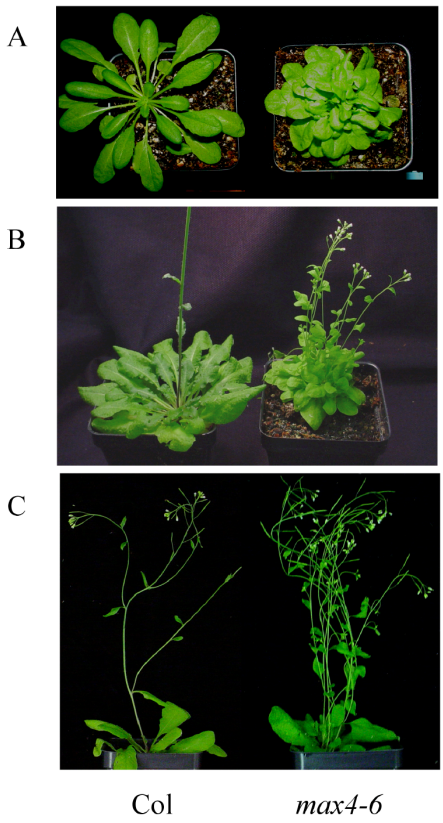

Figure 4-8. Phenotypes of *max4-6* plant compared to wild-type (Col). Plants grown in a short day light schedule (A and B) appeared to have an exaggerated phenotype compared to plants grown in a long day light schedule (C).

Table 4-2. Petiole and leaf blade lengths and inflorescence number (±SE) taken from plants grown on short and long days.

	Petiole (mm)		Leaf Blade (mm)		Inflorescence #	
Day Length	Short	Long	Short	Long	Short	Long
Ws	15.4±1.3	15.5±0.8	13.9±0.9	14.8±1.4	1.1±0.1	1.8±0.4
max4-5	10.4±0.6*	8.3±0.2*	16.8±0.8*	10.3±1.1*	10.0±2.1*	4.5±0.3*
Col	15.2±0.6	20.8±1.9	14.6±1.2	18.0±0.9	1.0±0.0	1.8±0.3
max4-6	11.4±0.5*	10.3±0.6*	9.8±0.5*	13.8±0.5*	10.5±1.7*	5.2±0.4*
CCD8OE*max4-6*	——	18.0±2.2	——	20.0±2.0	——	1.8±0.3

into *max4-6*. Transformed plants were grown on selection plates. Positive plants (*max4-6:CCD8*OE) were taken to homozygosity and were grown alongside *max4-6* and wildtype plants in a long day light schedule. The *max4-6:CCD8*OE line used for analysis showed a 3:1 segregation pattern at the T_2 generation indicating the existence of either

one or multiple linked newly introduced T-DNA(s). The phenotypes associated with petiole length, leaf blade length, and inflorescence number were all rescued (Table 4-2). *CCD8* transcript abundance was checked by Real Time RT-PCR in *max4-6:CCD8*OE plants and was interestingly only half of what is seen typically in wild-type plants. Complementation with sub-wild-type levels of transcript suggests that only a low level of *CCD8* expression is required. The complementation establishes that the phenotypes were a result of the loss of CCD8 function.

Determination of Indole Acetic Acid and Abscisic Acid Content within *max4-6* Plants

Like *max3*, *max4* alleles were found to have an altered branching pattern. This phenotype again evokes images of auxin biosynthetic and/or signaling mutants. Therefore, the level of auxin in the form of free IAA was measured. IAA levels were equal to wild-type (Fig. 4-9). CCD8 was also tested for its possible involvement in ABA production by ascertaining ABA content with the *max4-6* mutant and comparing it to wild-type. ABA levels were equal to wild-type (Fig. 4-9). Therefore, CCD8 also does not play a role in ABA synthesis.

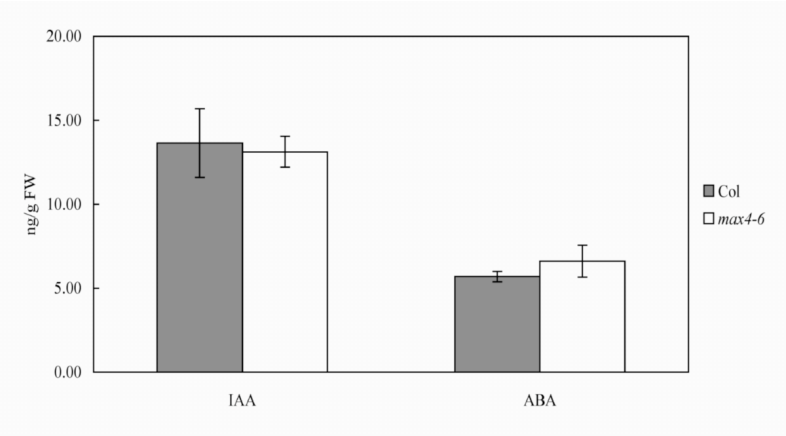

Figure 4-9. IAA and ABA content in *max4-6* rosettes compared to wild-type (Col). No difference in either hormone was seen.

In Summary

A recent study indicated that CCD8 has activity at the 13,14 double bond of 10'-apo-β-carotene, a product resulting from the activity of CCD7 on β-carotene (Schwartz et al., 2004). CCD8 is a plastid, specifically stroma, localized protein. Its transcript was most prominent in root tissue but was detectable in all other tissues tested. *CCD8* expression was not affected by day length or water stress. Two independent *CCD8* loss-of-function alleles exhibit the same phenotype characterized by increased branching and decreased petiole and leaf blade (with the exception of *max4-5* on short days) lengths. These phenotypes are similar to those seen in the *CCD7* loss-of-function mutants. CCD7 and CCD8 are non-redundant carotenoid cleavage dioxygenases required for the production of an apocarotenoid, which either directly or indirectly controls shoot growth from axillary meristems.

CHAPTER 5
GENETIC INTERACTION AMONG CCD1, CCD7, AND CCD8

Introduction

CCD1 and CCD7 share activity at the 9,10 double bond of linear and cyclic carotenoids (Schwartz et al., 2001; Booker et al., 2004; Schwartz et al., 2004). CCD7 and CCD8 share similar phenotypes conferred by their loss-of-function (Sorefan et al., 2003; Booker et al., 2004). To ascertain the genetic interaction between the CCDs, the following crosses were performed, *ccd1* x *max4* and *max3* x *max4*. A cross between *ccd1* and *max3* was also done, the progeny of which are at the F_1 generation and as such are not ready to be analyzed. The following two sections characterize the *ccd1max4* and *max3max4* double mutants by comparing them to wild-type and to each single mutant. The final section discusses results on transcript abundance of each CCD found within the CCD loss-of-function mutants.

Characterization of *ccd1max4* Plants

CCD1 and CCD8 do not appear to have much in common with the exception that CCD8 cleaves a 9,10 cleavage product of β-carotene. CCD8 cleaves at the 13,14 double bond of 10'-apo-β-carotene, an apocarotenoid produced by the 9,10 cleavage of β-carotene. No 10'-apo-β-carotene accumulated in the reactions involving CCD1 with β-carotene as a substrate. Instead the C_{14} dialdehyde corresponding to the central portion of β-carotene was identified, leading to the hypothesis that CCD1 may act as a dimer (Schwartz et al., 2004). It is not known if dimerization of CCD1 occurs *in vivo*. If CCD1 is able to cleave asymmetrically, two interactions with CCD8 are possible. One reaction

would begin with the cleavage of β-carotene by CCD1, the products of which are then cleaved by CCD8, much like the reactions involving CCD7. This is not likely due to the differential subcellular localization of CCD1 and CCD8. However, a second possibility remains in which β-carotene is cleaved by CCD7 to produce 10'-apo-β-carotene which is cleaved by CCD8 to produce 13'-apo-β-carotene. 13'-apo-β-carotene may leave the plastid and be cleaved by CCD1 at its one 9,10 double bond. The biological significance of this is unknown and may be revealed by the *ccd1max4* double mutant. *ccd1-1* showed a subtle petiole phenotype (Chapter 2). The *max4* background may provide a sensitized background in which to uncover further *ccd1* related phenotypes.

Due to constraints of selectable markers, the *max4* allele chosen to cross to *ccd1-1* was *max4-5*. The *max4-5* allele is in the Ws background and the *ccd1-1* allele is in the Columbia background. Comparisons were therefore made among each wild-type background, the single mutants, and the double mutant. Petiole length, leaf blade length and inflorescence number are shown in Fig. 5-1. Unfortunately, petiole and leaf blade length vary between Col and Ws making any conclusion regarding the effect of the double mutant difficult. The inflorescence number of Ws and Col was similar. The *ccd1max4* double mutant was no different in inflorescence number than *max4*. The introduction of *ccd1-1* into the *max4-6* background had no effect on shoot growth from axillary meristems suggesting that CCD1 is not involved in the control of branching in Arabidopsis.

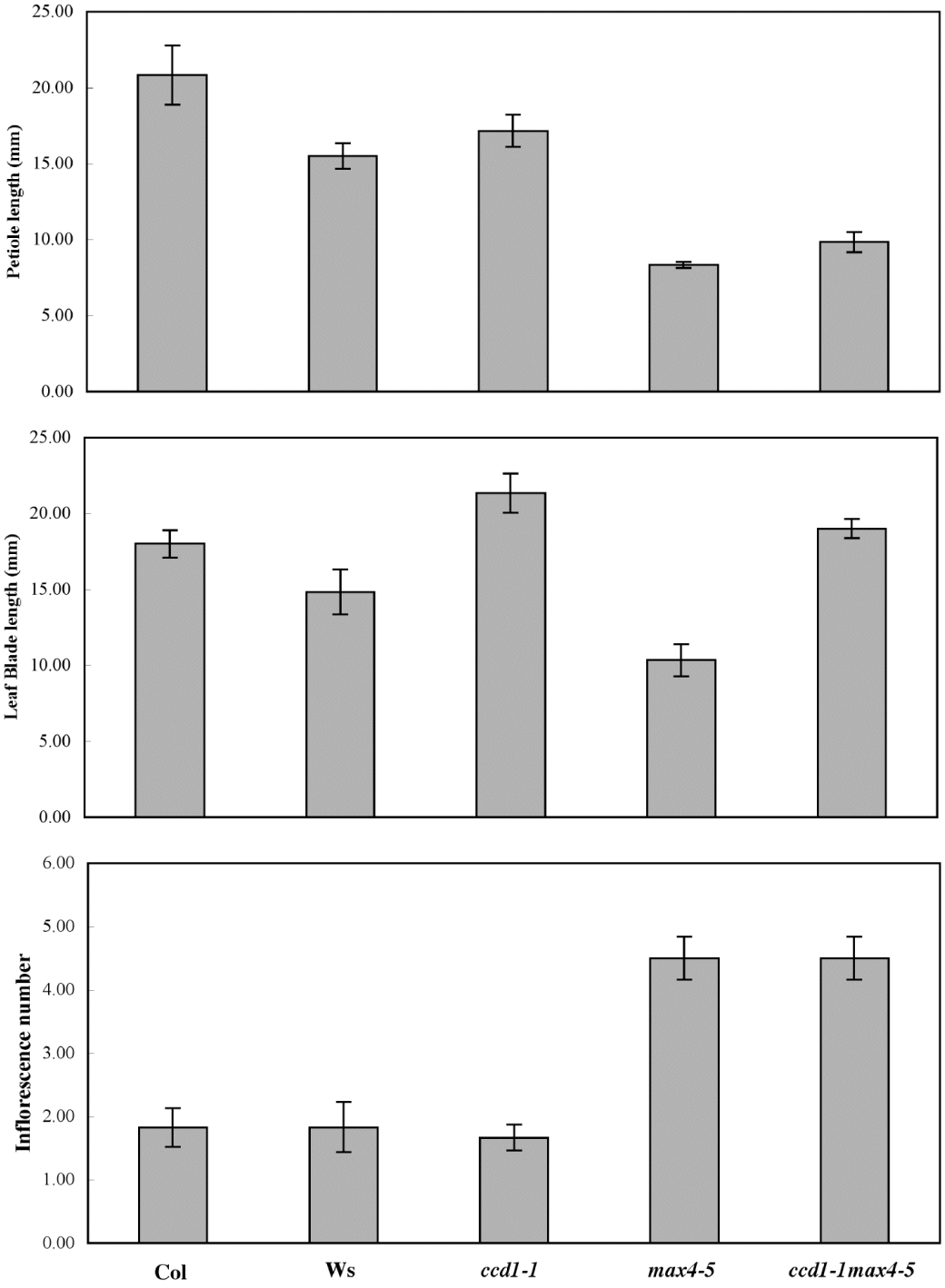

Figure 5-1. Analysis of *ccd1max4* double mutant. Measurements recorded include petiole and leaf blade lengths and inflorescence number.

Characterization of *max3max4* Plants

The near identical phenotypes of the *max3* and *max4* mutants suggests a pathway leading to the production of a branch controlling factor (Sorefan et al., 2003; Booker et al., 2004). It is possible that CCD7 and CCD8 work in a single pathway leading to the synthesis of an inhibitor of bud outgrowth in Arabidopsis. It is also possible that CCD7 and CCD8 act in independent pathways both of which contribute to the production of a branch inhibiting compound(s). If the latter were true, then a double *max3max4* mutant may be predicted to have an additive phenotype compared to either single mutant. Therefore, a cross between *max3-11* and *max4-6* was made. The double mutant will also give *in vivo* evidence for the existence of a linear pathway containing CCD7 and CCD8. The F_2 generation of the *max3-11 max4-6* cross was analyzed for petiole length, leaf blade length, and inflorescence number (Fig. 5-2). Genotypes were ascertained by PCR. Petiole length was shortest in *max4-6* and the double mutant. Only one copy of *CCD8* was required for wild-type petiole length as shown in the plants genotyped as heterozygous for *CCD8* (*max3*/+, *max4*/+ and *MAX3*/*MAX3*, *max4*/+). Leaf blade length was indistinguishable among *max3-11*, *max4-6* and *max3-11max4-6*. The *max3-11max4-6* double mutant was also phenotypically indistinguishable from either single mutant in inflorescence number indicating a lack of genetic interaction between CCD7 and CCD8 consistent with both genes functioning in the same pathway. Interestingly, both classes of plants genotyped as heterozygous for *CCD8* (*max3*/+, *max4*/+ and *MAX3*/*MAX3*, *max4*/+) showed a slight increase in inflorescence number compared to wild-type (P-value=0.076 and P-value=0.029, respectively). This evidence of a quantitative dosage

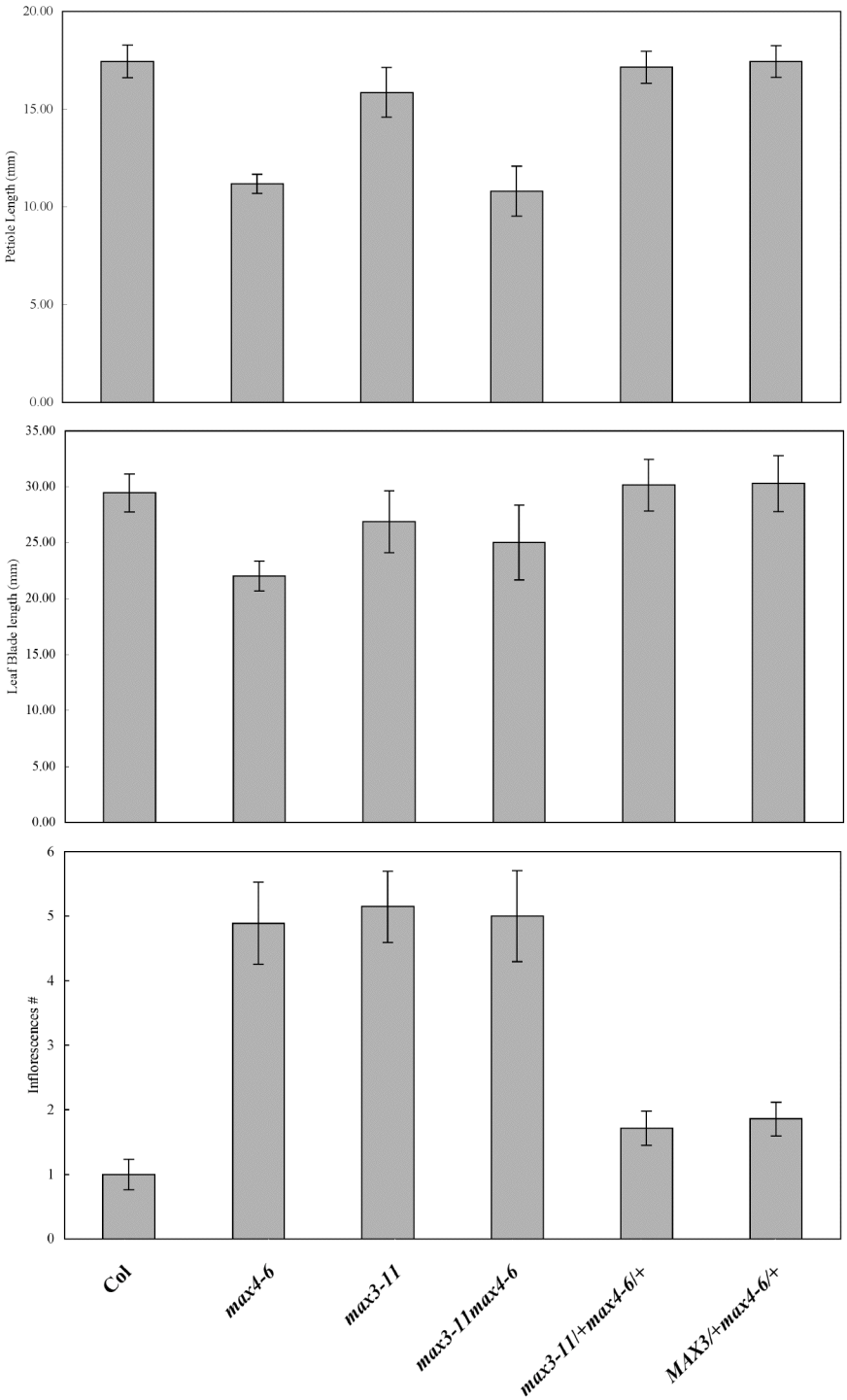

Figure 5-2. Analysis of *max3max4* double mutant. Two classes of heterozygotes, heterozygous at both loci (*max3-1/+max4-6/+*) and heterozygous at CCD8 *MAX3/+max4-6/+*) were included to show possible dosage effect of *CCD8*.

effect of *CCD8* on inflorescence number suggests that CCD8 activity is a point of control in the pathway.

Effect of Loss-of-Function Mutants on Expression of CCDs

Due to the biochemical overlap of CCD1 and CCD7 and to the placement of CCD7 and CCD8 in the same biosynthetic pathway, transcriptional regulation of one CCD on another was tested. Real Time RT-PCR was used to measure transcript abundance of each CCD in the *ccd1-1*, *max3-11*, and *max4-6* mutant backgrounds. Expression was measured at the seedling stage in two tissue types. The seedlings were extracted from plates and cut at the root hypocotyl junction to provide root sample and an aerial tissuesample consisting of hypocotyls and cotyledons (H/L). No large differences in expression were seen (Fig 5-3). However a few subtle changes should be noted. *CCD1* expression was decreased in the *max3* and *max4* mutants as compared to wild-type. *CCD7* expression was unchanged significantly in the root tissue of either *ccd1* or *max4* seedlings but was decreased in *ccd1* and *max4* H/L tissue. *CCD8* transcript on the other hand was decreased in *max3* root and H/L tissue. *CCD8* expression was also decreased in *ccd1* H/L tissue.

It is unclear whether there is an interaction between CCD1 and CCD7 or CCD8. The role of CCD1 in plant physiology is also unclear but as a carotenoid cleavage dioxygenase present in the cytoplasm it is feasible CCD1 acts as a vehicle for recycling of carotenoid backbones from degenerated chloroplasts. If this is the case, plants with increased branch number may need more photosynthates than less branched plants. A larger store of carotenoids may allow for an increased photosynthetic rate. So, the decrease in *CCD1* expression seen in the *max3* and *max4* mutants may be a consequence

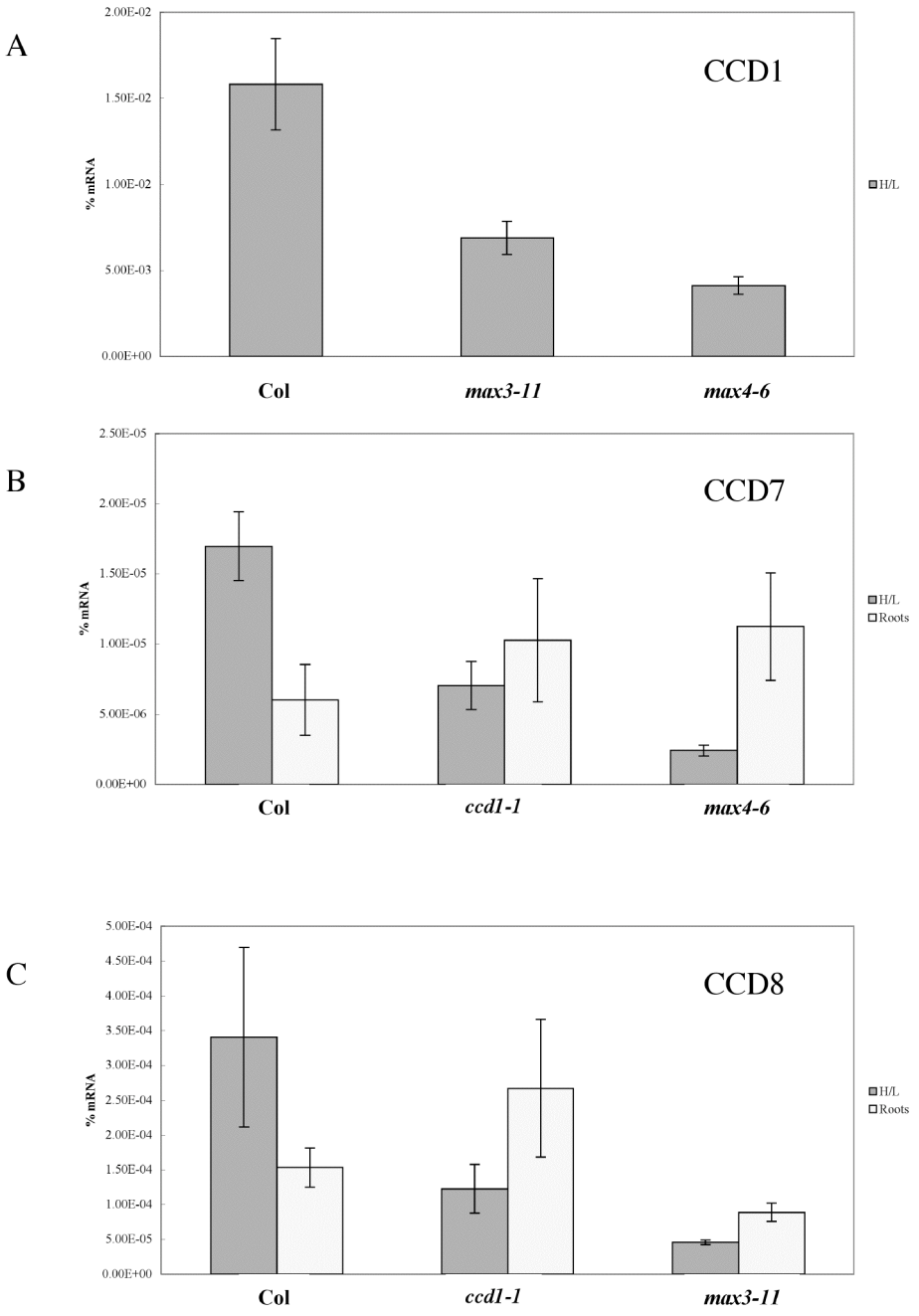

Figure 5-3. Effect of loss-of-function mutants on transcript abundance of CCD1 (A), CCD7 (B), and CCD8 (C).

of the *max* phenotype. It is strange that the change in *CCD7* expression among the mutant phenotypes was seen in H/L tissue instead of the root tissue, where in adult plants *CCD7* transcript is highest. Nonetheless the decrease of *CCD7* transcript in *max4*

seedlings may point to a negative feedback regulatory mechanism. Furthermore, *CCD8* transcript in *max3* was decreased in both root and H/L tissue. *CCD8* transcript was also decreased in *ccd1* H/L tissue.

CHAPTER 6
DISCUSSION

Introduction

The Arabidopsis CCD family consists of enzymes which not only range in substrate specificity and site of cleavage but also biological function. The NCEDs all cleave 9-cis-epoxycarotenoids at the 11,12 double bond to produce the hormone, ABA. CCD4 may cleave at the 5,6 double bond to produce volatile apocarotenoids which contribute to floral scent and to the flavor of fruits and vegetables (Winterhalter and Rouseff, 2002). CCD1 cleaves multiple carotenoid substrates symmetrically at their 9,10 (and 9',10') double bonds. With β-carotene as a substrate, CCD1 activity produces two β-ionone molecules (Schwartz et al., 2001). This is an apocarotenoid which has also been linked to floral aroma and flavor (Winterhalter and Rouseff, 2002). CCD7 has been shown to cleave multiple substrates at the 9,10 double bond (Booker et al., 2004). CCD7's biological function in plants is intriguing and appears to be linked with the activity of CCD8. CCD7 and CCD8 are required for the production of a novel signaling molecule which is involved in the inhibition of branching (Sorefan et al., 2003; Booker et al., 2004) but whose chemical identity has yet to be established. The following discussion on results presented thus far is divided into two sections, the first pertains to CCD1 in terms of its possible biological roles in plant physiology and the second combines CCD7 and CCD8 regarding their involvement in the production of a novel signaling compound.

Carotenoid Cleavage Dioxygenase 1

It is difficult to assign a specific biological function to CCD1 because of its substrate promiscuity. However, the *in vitro* activity of CCD1 on β-carotene does produce β-ionone and a C_{14} dialdehyde, both of which are known to contribute to floral scent and fruit flavor (Winterhalter and Rouseff, 2002). CCD1 expression was high in flowers as compared to other plant organs. The volatile compounds may act to attract insects for pollination as compounds such as β-ionone have been shown to lure insects to traps containing mixtures of β-ionone with other known volatile compounds from maize (Hammack, 2001). Pollination by insects is most probably not a typical means of fertilization for a self-pollinating plant like Arabidopsis. However, it may be beneficial to a plant like Arabidopsis to maintain a means by which diversity in genetic makeup could be obtained (Chen et al., 2003). Apocarotenoids have antifungal activities as well. When the roots of maize and wheat are infected with arbuscular mycorrhizal fungi, cyclic C_{13} compounds and acyclic C_{14} compounds accumulate, giving the roots a yellow color. The function of the carotenoid precurors and the apocarotenoid products in arbuscular mycorrhization is unknown. However, it is possible that apocarotenoids act to control fungal colonization because application of the isoprenoid cleavage product, blumenin, deters colonization (Fester, 1999).

As carotenoids are synthesized and for the most part reside in plastids, it seems strange that a carotenoid cleavage dioxygenase not localized to the plastid exists. However, CCD1 clearly shows CCD activity but was not found to be plastid-localized. The presence of carotenoids in the outer envelope of the chloroplast has been reported in spinach (Douce et al., 1973) and pea (Markwell et al., 1992). The envelope fraction from

spinach contained mostly violaxanthin but lutein and zeaxanthin and in smaller quantities -carotene were also isolated (Douce et al., 1973). All of these carotenoids are possible CCD1 substrates (Schwartz et al., 2001). CCD1 may associate with the outer envelope and act on the carotenoids found within it. In fact, a CCD1 orthologue from tomato was found in fractions containing the inner and outer chloroplast envelopes but was easily degraded by treatment with a protease (Simkin et al., 2004a). Extensions of the plastid membrane have also been discovered. Thought to take part in protein exchange between plastids (Kohler et al., 1997), these stroma filled tubules may also be a source of carotenoids available to CCD1.

The subtle phenotype seen in *ccd1-1* suggests that CCD1 may not be crucial to normal growth and development or that redundancy exists in the genome. CCD7 does possess the same cleavage activity as CCD1 yet they differ in their subcellular localization. Was CCD1 at one point redundant to CCD7 but through evolution lost its chloroplast transit sequence? Would CCD1 be able to rescue the *max3* phenotype if present within plastids? To answer these questions the transit peptide of the plastid localized small subunit of ribulose 1,5 carboxylase/oxygenase was placed in front of CCD1. The construct encoding for the chimeric protein was transformed into *max3-9* plants. In a reciprocal experiment, the transit peptide-coding region of *CCD7* was removed and put into *max3-9* plants to test if plastid localization is in fact a requirement for rescue of the *max3* phenotype. Analysis of the resulting plants is in progress.

Carotenoid Cleavage Dioxygenase 7 and Carotenoid Cleavage Dioxygenase 8

Traditionally, apical dominance is thought of as a consequence of the effects of two plant hormones, auxin and cytokinins. It has been postulated that auxins, produced in the

apex of the plant, travel down the stem and inhibit growth of axillary meristems (Ward and Leyser, 2004). With the isolation of the *max3* and *max4* mutants, an as yet unidentified hormone player in the control of plant architecture is evident (Stirnberg et al., 2002; Sorefan et al., 2003; Booker et al., 2004). Studies in pea (*Pisum sativum*) (Beveridge et al., 1996; Beveridge et al., 2000; Morris et al., 2001; Rameau et al., 2002), and petunia (*Petunia hybrida*) (Napoli, 1996) (K. Snowden, personal communication) also point to a more complex mechanism controlling branching in plants. In each of these species phenotypes identical to that seen in the Arabidopsis loss-of-function mutants were discovered, demonstrating that this is a general phenomenon. Prominent among these studies were those done with the *ramosus* (*rms*) mutants in pea. There are six identified *RMS* loci. Mutations in any of the six loci confer an increased branching pattern. This phenotype exists despite the mutants possessing wild-type auxin content and transport (Beveridge et al., 2000; Morris et al., 2001; Rameau et al., 2002). Recently, it was shown that PsRMS1 is orthologous to AtCCD8 (Sorefan et al., 2003). As reported here, the *max4-6* mutant, like *rms1*, also contains wild-type levels of auxin. However, auxin sensitivity may be altered as it was decreased in the *max4-1* mutant (Sorefan et al., 2003) indicating a potential link to auxin signaling.

Grafting studies done in both Arabidopsis (Turnbull et al., 2002; Sorefan et al., 2003) and pea (Foo et al., 2001) further implicate CCD7 and CCD8 and their orthologues in branching inhibition. In Arabidopsis, the *max4* branching phenotype can be restored to wild-type by grafting at the seedling stage with either wild-type root or shoot tissue (Sorefan et al., 2003). Similar results have been reported for *max3* (Turnbull et al., 2002) and *rms1* (Foo et al., 2001). Y grafts, in which a shoot of one genotype is grafted onto

the shoot of a second genotype, were performed using *rms1* and wild-type tissue. Here, an *rms1* shoot was grafted onto a wild-type shoot continuous with a wild-type root. Neither shoot developed excessive branching. On the other hand, when the wild-type shoot was grafted onto an *rms1* shoot that was continuous with an *rms1* root, the *rms1* shoot but not the wild-type shoot developed extensive branching. These data show that the signal travels acropetally and therefore is more than likely transported through the xylem (Foo et al., 2001). Although *CCD7* and *CCD8* transcripts were present in all tissues they are, by far, most highly expressed in the roots. Sorefan et al. showed highest expression of *CCD8* in the root tip using promoter GUS fusions (Sorefan et al., 2003). The available data strongly support the existence of a novel translocated phytohormone able to travel up through the xylem from the root to affect shoot branching.

Branching mutants have also been identified in petunia. The *dad1* mutant was characterized as having an increased branching pattern (Napoli, 1996) and Dad1 has now been shown to be orthologous to AtCCD8 (K. Snowden, personal communication). Orthologous proteins controlling identical functions as well as the existence of homologous sequences in the monocots maize and rice (B.C. Tan and D. R. McCarty, personal communication) indicate a broadly conserved mechanism for controlling lateral branching in plants.

The order of action of CCD7 and CCD8 in this pathway is not known. Both CCD7 (Chapter 3) (Booker et al., 2004) and CCD8 (Chapter 4) localize to the stroma of chloroplasts, placing them in a cellular compartment that is enriched for carotenoids. CCD7 has been shown to cleave a variety of carotenoid molecules (Booker et al., 2004)

whereas cleavage activity of CCD8 has been suggested using 10'-apo-β-carotene as a substrate (Schwartz et al., 2004).

Other participants in this pathway to date remain unidentified. However, two additional branching mutants in Arabidopsis, *max1* and *max2*, have been identified but their role in the synthesis of the branch inhibiting compound is not yet known (Stirnberg et al., 2002). Six RMS loci have been identified in pea (Beveridge et al., 1996; Beveridge et al., 2000; Morris et al., 2001; Rameau et al., 2002). Reciprocal grafting experiments among the *rms* mutants show Rms3 and Rms4 to be more important in the shoot than in the root. Rms1 and Rms 5 appear to regulate the same signal emanating from the root (Morris et al., 2001) and Rms2 has been hypothesized to act as a shoot to root signal (Beveridge, 2000). From these studies it is obvious that branching control is regulated by a complex signaling network. To add to this complexity the recently discovered *BYPASS1 (BPS1)* was also shown to be involved in the control of apical growth. BYPASS1 does not possess strong homology to any known protein. Mutants of *BPS1* do not grow past the production of two cotyledonary leaves, which have no vasculature or trichomes. *bps1* plants also display a short root phenotype. The *bps1* phenotypes are temperature sensitive in that they become less severe with increasing temperature. Interestingly a partial rescue of *bps1* phenotypes are seen with fluridone treatment. Fluridone inhibits phytoene desaturase and therefore carotenoid biosynthesis. Furthermore, the *aba1bps1* double mutant showed an enhanced *bps1* phentoype. ABA1 converts zeaxanthin to violaxanthin. These results led authors to hypothesis the existence of a zeaxanthin-derived signal regulated by BPS1, which inhibits apical growth (Van Norman et al., 2004). CCD7 and CCD8 may be responsible for the synthesis of this

carotenoid derived signaling molecule, without which apical growth is left uninhibited leading to the highly branched phenotypes seen in *max3* and *max4*. The isolation of *max*, *rms*, *dad* and now *bps1* strongly suggest that a carotenoid derived compound is a novel growth inhibiting phytohormone, which along with auxins and cytokinins represent a means by which plants control their pattern of growth.

CHAPTER 7
MATERIALS AND METHODS

Cloning of *CCD1*, *CCD7* and *CCD8* cDNA

CCD1

The *CCD1* cDNA in pBK-CMV (Stratagene, La Jolla, CA) was a gift from B. C. Tan. *CCD1* cDNA was put into the Gateway pENTRD (Invitrogen, Carlsbad, CA) using the following primers; Forward 5'-caccatggcggagaaactcagtatggcag-3' and Reverse 5'-ttatataagagtttgttcctggagttgttc-3' and sequenced. From pENTRD, *CCD1* cDNA was transferred to pDESTOE (Booker et al., 2004) by recombination for overexpression. The pDESTOE vector contains the constitutive Figwort Mosaic Virus promoter and NOS terminator as well as the plant selection gene, *nptII*. *CCD1*pBK-CMV was digested with *Pst*I/*Sma*I and ligated into pSP6-PolyA (Promega, Madison, WI) for *in vitro* transcription and translation.

CCD7

The *CCD7* cDNA was obtained by a two-step RT-PCR reaction with RNA from Columbia tissue. Advantage RT-for-PCR reagents (BD Biosciences Clontech, Palo Alto, CA) were used according to the manufacturer and *CCD7* was amplified from cDNA using the following primers; Foward 5'-caccatggcggagaaactcagtgatggcag-3' and Reverse 5'-ttatataagagtttgttcctggagttgttcctgtgaatacc-3'. Full length cDNA was maintained in either the pCR-BluntII-TOPO vector or the pENTRD vector (both from Invitrogen) and sequenced. *CCD7* cDNA was transferred from *CCD7*pENTRD to pDESTOE (Booker et al., 2004) for overexpression by recombination, to pDEST14 (Invitrogen) for expression

by recombination, and to pSP6-PolyA (Promega) by digestion with *Pst*I and *Sac*I for *in vitro* transcription and translation.

CCD8

The *CCD8* cDNA in pBlueScript (KS) was a gift from Steve Schwartz. A single nucleotide mutation was found in the cDNA clone and corrected using a BD Biosciences Clontech mutagenesis kit. The sequence matched that of the annotated gene in GenBank (At4g32810). *CCD8* cDNA was amplified using the following primers F 5'- caccatggcttctttgatcacaaccaaagc- 3', R 5'- ttaatctttggggatccagcaaccatg-3', put into the Gateway pENTR2B vector (Invitrogen) and sequenced. *CCD8* cDNA was transferred from *CCD8*pENTR2B to pDESTOE (Booker et al., 2004) for overexpression by recombination and to pSP6-PolyA (Promega) by digestion with *Sal*I and *Xba*I for *in vitro* transcription and translation..

Carotenoid/Apocarotenoid Extraction from *E.coli*

Plasmids containing the carotenoid biosynthetic genes (courtesy of F. Cunningham) for phytoene, β-carotene, lycopene, β-carotene, β-carotene, and zeaxanthin were co-transformed with *CCD7*pDEST14 into the arabinose inducible *E. coli* strain, BL21-AI (Invitrogen). Cells were grown in LB with 0.1% glucose at 30^{O}C for varying amounts of time depending on the extraction procedure. Expression of *CCD7* was induced by the addition of 0.1% arabinose when cells reached an A_{600} of 1.0.

For HPLC analysis, one preculture was grown and used to inoculate two 25 ml cultures, one of which was induced for CCD7 expression once an A_{600} of 1.0 was reached. The 25 ml cultures were grown for an additional 24 h and carotenoids were extracted using the method of Fraser et al. (Fraser et al., 2000). Injection volumes for

extracts from uninduced and induced cells were normalized for A_{600} taken just prior to extraction to directly compare accumulation of the carotenoid substrate. Analysis was carried out on a Waters (Milford, MA) HPLC, equipped with a photodiode array detector and a reversed-phase YMC Carotenoid S-5 4.6x250 mm column (Waters). HPLC running parameters are as described in (Fraser et al., 2000). The apocarotenoid products were detected by gas chromatography and verified by gas chromatography/mass spectrometry, by the running parameters of (Engelberth et al., 2003). For apocarotenoid analysis, cell cultures (25 ml) were grown for no more than 12 h and apocarotenoids were extracted by the addition of an equal volume of hexane. Culture/hexane solutions were sonicated in a water bath sonicator for 5 m and vortexed for 1 m. The phases were separated by centrifugation and the hexane phase was retained. Apocarotenoid volatiles were collected onto a filter trap (containing 20 mg of SuperQ, Alltech Associations) by vapor-phase extraction as described in (Engelberth et al., 2003), with the exception that samples were dried to completion then heated to 75^{O}C to promote volatility. For the β-carotene strain, a 100 ml culture was grown for 16h. Air was bubbled through the culture and volatiles were collected onto the SuperQ filter trap. In both apocarotenoid extraction procedures, volatiles were eluted off the trap with 150 µl of hexane, of which 5 µl were injected onto the GC. Injection volumes for extracts from uninduced and induced cells were normalized for A_{600}.

Plant Growth Conditions and Measurements

Plants were grown under Cool White and Gro-Lux (Sylvania) fluorescent tubes at 50 µmol m^{-2} s^{-1}. Temperatures ranged from 19^{O}C to 22^{O}C. Short days consisted of 8 h light and 16 h dark, while long days consisted of 16 h light and 8 h dark. Measurements of

petiole length and leaf blade length were taken from the 6th leaf on the rosette. A combined inflorescence number was obtained by counting every inflorescence, emerging from the primary meristem and axillary meristems, one week in long days and two weeks in short days after observation of primary inflorescence emergence. For all measurements, data from at least 6 plants were averaged.

Subcellular Localization

TNT

Transcription of each cDNA was under the control of the SP6 promoter in the pSP64-PolyA vector (Promega). *In vitro* transcription and translation was done using the coupled transcription/translation (TNT) wheat germ extract (for CCD1 and CCD8) or the rabbit reticulocyte lysate (for CCD7) system by Promega. A 100 µl reaction contained the following ingredients, 50 µl wheat germ extract or rabbit reticulocyte lysate, 4 µl TNT reaction buffer, 2 µl SP6 RNA polymerase, 2 µl amino acid mixture minus leucine, 28 µl ^{3}H-leucine, ribonuclease inhibitor (20 units/ml), and 6 µg of plasmid DNA. Reactions were incubated for 30m at 25^{0}C. A 2 µl aliquot of TNT reaction products was set aside and the remaining reaction mix was brought to 200 µl with 60 mM leucine in 2X import buffer (IB) (1X IB = 50 mM HEPES/KOH pH 8.0, 0.33 M sorbitol).

Chloroplast Import

Chloroplasts were isolated from 9-11 day old pea seedlings (Laxton's Progress 9). Import assays were performed as described by Cline et al. (1993). Import assays were set up as follows, 200 µl precursor protein (TNT reaction products) were added to 200 µl chloroplasts (resuspended to ~1.0 mg Chlorophyll/ml), 25µl 120mM Mg-ATP in 1X IB pH8.0, 30 µl 0.1 M DTT, and 145 µl 1X IB. Import was allowed to proceed for 30 m at

25^{O}C under light and stopped by transferring tubes to ice. Chloroplasts were pelleted (1000xg for 6 m) and resuspended in 0.5 ml import buffer. Chloroplasts were then treated with 25 µl thermolysin (2 mg/ml in IB, 10 mM $CaCl_2$). Thermolysin treatment proceeded for 40 m at 4^{O}C. Chloroplasts were then repurified on a 35% Percoll cushion, washed with 1X IB, and resuspended in 10 mM Hepes-KOH/5 mM EDTA pH 8.0.

Subfractionation

Following import, chloroplasts were repurified on a 35% Percoll cushion, washed with 1X IB, lysed by resuspension in 10 mM Hepes-KOH/5 mM EDTA pH 8.0 and allowed to sit on ice for 5 m. To adjust the osmolarity of the solution, 20 µl of 2X IB/20 mM $MgCl_2$ was added. Thylakiods were isolated by spinning chloroplasts at 4000xg for 30 s at 4^{0}C. The pellet was washed with 1ml 1X IB, spun at 8200 g for 3 m, and resuspended in 120 µl 10 mM Hepes-KOH/5 mM EDTA pH 8.0. The supernatant was removed and spun for 30 m at 50,000xg at 2^{0}C to separate envelope inner and outer membranes from stroma. The supernatant (stromal fraction) was removed and the volume carefully measured. The pellet (envelope fraction) was resuspended in the same volume as the stromal fraction with 10 mM Hepes-KOH/5 mM EDTA pH 8.0.

Thermolysin treated whole chloroplasts and chloroplast subfractions were mixed with 2X SDS sample buffer, heated to 80^{0}C for 3 m, and run out on 12.5% SDS-polyacrylamide gels. The gels were incubated in DMSO for 5 m with shaking and then with enough 2,5-diphenyloxazole (PPO) in DMSO to cover the gel for 30 m with shaking. After washing in water, the gels were dried and the proteins were detected by fluorography.

Real Time RT-PCR

To determine the major sites of *CCD* expression, tissues for RNA were harvested from Columbia plants grown in soil on short days for 2.5 months. Plants were then switched to long days in order to promote flowering. Once plants bolted, primary inflorescence stem (primary inflorescence minus flowers and cauline leaves), flower and green silique tissues were collected. Secondary inflorescence stems were collected once they reached 8 cm in height. Primary inflorescence stem is the shoot originating from the primary shoot meristem whereas secondary inflorescence stems are the shoots originating from the axillary meristems. Total RNA was isolated as described in Chang et al. (1993). Tissue expression patterns were determined for three biological replicates. Data for one replicate is shown. Relative expression patterns for each replicate were equivalent.

To determine day length effect on gene expression, RNA was harvested from 14 day-old seedlings. Two sets of seedlings were grown on agar plates containing Murashige and Skoog basal salt mixture (Sigma-Aldrich, St. Louis, MO) for 14 days on a short day light schedule, at which time half of the plates were switched to long days. Eight days later, both sets were collected and frozen and RNA was harvested. Averages and standard errors of three replicates are shown.

For analysis of the effect of water stress on *CCD* expression, tissue was collected from 14 day-old seedlings (short day light cycle) harvested from MS plates and left on the bench until they lost 15% of their fresh weight. They were then sealed in plastic bags and put in the dark for 6 h. Nonstressed tissue was harvested in the same way but was sealed in plastic bags immediately after removal from plates, kept in the dark for 6 h, then

frozen and RNA extracted. The above procedures are also detailed in Tan et al. (2003). Averages and standard errors of three replicates are shown.

All RNA was DNaseI (Ambion, Austin, TX) treated at 37^{O}C for 30 m. DNase was removed using the RNeasy kit from Qiagen (Valencia, CA). RNA was visualized on agarose gels and quantified by spectrophotometry. An Applied Biosystems GeneAmp 5700 real-time PCR machine was used with TaqMan One-Step RT-PCR reagents (Applied Biosystems, Foster City, CA) and reaction conditions were as per manufacturer specifications using 250 ng RNA per reaction in a 25 □l reaction volume. Reactions were done in duplicate and quantities were averaged. The primer/probe set for each CCD are shown in Table 7-1. Transcript quantities were determined by comparison to a standard curve. Transcripts for use in production of standard curves were synthesized with T7 polymerase *in vitro* in the presence of [^{3}H]-UTP from *CCD1*pBK-CMV (linearized with *Not*I), *CCD7*pBluntII (linearized with *Spe*I), and *CCD8*pENTR2B (linearized with *Xba*I). Quantities were then normalized to ribosomal RNA, which was detected using the Taqman Ribosomal RNA Control Reagents kit by Applied Biosystems.

Table 7-1. Primers used in Real Time RT-PCR reactions.

	Forward Primer 5'…3'	Probe 5'-FAME...TAMRA-3'	Reverse Primer 5'…3'
CCD1	acaagagattgacccactccttca	tgctcacccaaaagttgacccggt	tgtttacattcggctattcgca
CCD7	caaccgagtcaagcttaatcca	aggttccatagcggctatgtgcgga	aacgctgataccattggtgaca
CCD8	tgataccatctgaaccattcttcgt	5cctcgacccggtgcaacccat	cgatatcaccactccatcatcct

Isolation of Loss-of-Function Mutants

Three publically available populations were used to obtain mutants in this study, the Wisconsin Knock-out facility (Krysan et al., 1999; Weigel et al., 2000), the Syngenta

Arabidopsis Insertion Library (SAIL) (Sessions et al., 2002) and the Salk Institute Genomic Analysis Laboratory (Alonso et al., 2003). Each population is a collection of mutants obtained via *Agrobacterium*-mediated insertional mutagenesis. The mutants resulting from this form of mutagenesis, which no longer express the gene of interest, are called knock-outs because either their promoter or coding region is disrupted by the T-DNA insert (Krysan et al., 1999). At the time the mutants in this study were isolated the Wisconsin Knockout population organized their population of knock-outs in pools such that several, sequentially smaller pools must be screened before finding the one plant that is a knock-out for the gene of interest. Therefore, a pool of DNA was screened via PCR by the facility using primers listed in Table 7-2 and a primer specific for the left border sequence of the T-DNA (LB). Once supplied by the facility, PCR products were run out on an agrose gel and blotted for Southern analysis using full length cDNA clones as probes. Two populations from the Wisconsin Knock-out Facility exist, the Alpha (Krysan et al., 1999) and the Basta (Weigel et al., 2000) populations. Positive plants isolated from the Alpha population are resistant to kanamycin and those from the Basta population are resistant to glutamine synthetase inhibitors such as BASTA. The active ingredient in commercially available forms of BASTA is the glutamate analog, glufosinate-ammonium. Mutants from either the SAIL or Salk populations are obtained by searching a database for sequence matches. A positive match means that the population does contain a knock-out of your gene. The seeds are ordered and arrive as a segregating population. Recently, the Wisconsin Knock-out population and the SAIL population have been given to the Salk Institute Genomic Analysis Laboratory and are searchable through their database (signal.salk.edu).

For each population PCR was used to identify a plant homozygous for the T-DNA insert. Gene specific primers used in these reactions are listed in Table 7-2. Amplification with the forward and reverse gene specific primers indicated a wild-type copy. Amplification using either forward or reverse gene specific primer and the LB primer indicated the presence of a T-DNA within the gene.

Table 7-2. Gene specific primers used to identify knock-out plants

	Forward Primer	Reverse Primer
CCD1	5'-cagagtgttggatcgttgctggaagaaag-3'	5'-tcctggagttgttcctgtgaataccagac-3'
CCD7	5'-gctcatgtcttccacaaaatcactcaact-3'	5'-aaccatgaaaacccatcggaaacgtcaaa-3'
CCD8	5'-aaaaccgcatcaaaacttaccgtcaaact-3'	5'-ttgcgaattgataggtggaaccagtgaac-3'

β-ionone Measurements

Plants were grown on short days until rosettes contained from 22 to 27 leaves. Whole rosettes were ground individually under liquid N_2 and approximately 200 mg of each sample was used for extraction. β-ionone was extracted following the method of Schmelz et al. (Schmelz et al., 2003), with the following exceptions. The extraction solution used was 1-propanol/H_2O (2:1 vol/vol). Following shaking in a FastPrep FP 120 tissue homogenizer, hexanes were added to the samples and shaken again. The hexanes/1-propanol (top) phase was transferred to a new vial. No derivitization/neutralization step was necessary. β-ionone was collected by vapor-phase extraction as described in Schmelz et al. (2003). However, samples were heated to no higher than 70^{O}C until dry, then 2 m more. β-ionone was eluted from the filter trap with 150 µl of hexanes. Samples were injected onto a GC-MS, conditions of which are also

described in Schmelz et al. (2003). Sample β-ionone quantities were determined by an external standard curve.

IAA and Abscisic Acid Measurements

Wild-type and mutant plants were grown on short days until their rosettes contained 15-20 leaves, at which time rosettes were frozen individually. ABA and IAA were quantified following the procedure of Schmelz et al. (2003). Samples were injected onto a GC-MS, conditions of which are also described in Schmelz et al. (2003). Tissue from six rosettes was analyzed individually and the measurements were averaged.

LIST OF REFERENCES

Alonso JM, Stepanova AN, Leisse TJ, Kim CJ, Chen H, Shinn P, Stevenson DK, Zimmerman J, Barajas P, Cheuk R, Gadrinab C, Heller C, Jeske A, Koesema E, Meyers CC, Parker H, Prednis L, Ansari Y, Choy N, Deen H, Geralt M, Hazari N, Hom E, Karnes M, Mulholland C, Ndubaku R, Schmidt I, Guzman P, Aguilar-Henonin L, Schmid M, Weigel D, Carter DE, Marchand T, Risseeuw E, Brogden D, Zeko A, Crosby WL, Berry CC, Ecker JR (2003) Genome-wide insertional mutagenesis of Arabidopsis thaliana. Science **301:** 653-657

Aukerman MJ, Hirschfeld M, Wester L, Weaver M, Clack T, Amasino RM, Sharrock RA (1997) A deletion in the PHYD gene of the Arabidopsis Wassilewskija ecotype defines a role for phytochrome D in red/far-red light sensing. Plant Cell **9:** 1317-1326

Bak S, Tax FE, Feldmann KA, Galbraith DW, Feyereisen R (2001) CYP83B1, a cytochrome P450 at the metabolic branch point in auxin and indole glucosinolate biosynthesis in Arabidopsis. Plant Cell **13:** 101-111

Baldwin EA, Scott, J.W., Shewmaker, C.K., Schuch, W. (2000) Flavor trivia and tomato aroma: Biochemistry and possible mechanisms for control of important aroma components. HortScience **35:** 1013-1021

Beveridge C (2000) Long-distance signalling and a mutational analysis of branching in pea. Plant Growth Reg **32:** 193-203

Beveridge CA, Ross JJ, Murfet IC (1996) Branching in pea (Action of genes Rms3 and Rms4). Plant Physiol **110:** 859-865

Beveridge CA, Symons GM, Turnbull CG (2000) Auxin inhibition of decapitation-induced branching is dependent on graft-transmissible signals regulated by genes Rms1 and Rms2. Plant Physiol **123:** 689-698

Booker J, Auldridge M, Wills S, McCarty D, Klee H, Leyser O (2004) MAX3/CCD7 is a carotenoid cleavage dioxygenase required for the synthesis of a novel plant signaling molecule. Curr Biol **14:** 1232-1238

Bouvier F, Dogbo O, Camara B (2003a) Biosynthesis of the food and cosmetic plant pigment bixin (annatto). Science **300:** 2089-2091

Bouvier F, Suire C, Mutterer J, Camara B (2003b) Oxidative remodeling of chromoplast carotenoids: identification of the carotenoid dioxygenase CsCCD and CsZCD genes involved in Crocus secondary metabolite biogenesis. Plant Cell **15:** 47-62

Burbidge A, Grieve TM, Jackson A, Thompson A, McCarty DR, Taylor IB (1999) Characterization of the ABA-deficient tomato mutant notabilis and its relationship with maize Vp14. Plant J **17:** 427-431

Chang S, Puryear J, Cairney J (1993) A simple and efficient method for isolating RNA from pine trees. Plant Mol Biol Rep **11:** 113-116

Chatfield SP, Stirnberg P, Forde BG, Leyser O (2000) The hormonal regulation of axillary bud growth in Arabidopsis. Plant J **24:** 159-169

Chen F, Tholl D, D'Auria JC, Farooq A, Pichersky E, Gershenzon J (2003) Biosynthesis and emission of terpenoid volatiles from Arabidopsis flowers. Plant Cell **15:** 481-494

Chernys JT, Zeevaart JA (2000) Characterization of the 9-cis-epoxycarotenoid dioxygenase gene family and the regulation of abscisic acid biosynthesis in avocado. Plant Physiol **124:** 343-353

Cline K, Henry R, Li C, Yuan J (1993) Multiple pathways for protein transport into or across the thylakoid membrane. EMBO J **12:** 4105-4114

Cohen JD, Slovin JP, Hendrickson AM (2003) Two genetically discrete pathways convert tryptophan to auxin: more redundancy in auxin biosynthesis. Trends Plant Sci **8:** 197-199

Cunningham DG, Acree, T.E., Barnard, J., Butts, R., Braell, P. (1986) Analysis of apple volatiles. Food Chem **19:** 137-147

Cunningham FX, Gantt E (1998) Genes and enzymes of carotenoid biosynthesis in plants. Annu Rev Plant Physiol Plant Mol Biol **49:** 557-583

Cunningham FX, Jr., Pogson B, Sun Z, McDonald KA, DellaPenna D, Gantt E (1996) Functional analysis of the beta and epsilon lycopene cyclase enzymes of Arabidopsis reveals a mechanism for control of cyclic carotenoid formation. Plant Cell **8:** 1613-1626

Cunningham FX, Jr., Sun Z, Chamovitz D, Hirschberg J, Gantt E (1994) Molecular structure and enzymatic function of lycopene cyclase from the cyanobacterium Synechococcus sp strain PCC7942. Plant Cell **6:** 1107-1121

Devlin PF, Robson PR, Patel SR, Goosey L, Sharrock RA, Whitelam GC (1999) Phytochrome D acts in the shade-avoidance syndrome in Arabidopsis by controlling elongation growth and flowering time. Plant Physiol **119:** 909-915

Douce R, Holtz RB, Benson AA (1973) Isolation and properties of the envelope of spinach chloroplasts. J Biol Chem **248:** 7215-7222

Emanuelsson O, Nielsen H, Brunak S, von Heijne G (2000) Predicting subcellular localization of proteins based on their N-terminal amino acid sequence. J Mol Biol **300:** 1005-1016

Engelberth J, Schmelz EA, Alborn HT, Cardoza YJ, Huang J, Tumlinson JH (2003) Simultaneous quantification of jasmonic acid and salicylic acid in plants by vapor-phase extraction and gas chromatography-chemical ionization-mass spectrometry. Anal Biochem **312:** 242-250

Fester T, Maier, W., Strack, D. (1999) Accumulation of secondary compounds in barley and wheat roots in response to inoculation with an arbuscular mycorrhizal fungus and co-inoculation with rhizosphere bacteria. Mycorrhiza **8:** 241-246

Finkelstein RR, Gampala SS, Rock CD (2002) Abscisic acid signaling in seeds and seedlings. Plant Cell **14 Suppl:** S15-45

Foo E, Turnbull CG, Beveridge CA (2001) Long-distance signaling and the control of branching in the rms1 mutant of pea. Plant Physiol **126:** 203-209

Fraser PD, Pinto ME, Holloway DE, Bramley PM (2000) Technical advance: application of high-performance liquid chromatography with photodiode array detection to the metabolic profiling of plant isoprenoids. Plant J **24:** 551-558

Fray RG, Wallace, A., Fraser, P. D., Valero, D., Hedden, P., Bramley, P. M., Grierson, G. (1995) Constitutive expression of a fruit phytoene synthase gene in transgenic tomatoes causes dwarfism by redirecting metabloites from the gibberellin pathway. Plant J **8:** 693-701

Hammack L (2001) Single and blended maize volatiles as attractants for diabroticite corn rootworm beetles. J Chem Ecol **27:** 1373-1390

Havaux M (1998) Carotenoids as membrane stabilizers in chloroplasts. Trends Plant Sci **3:** 147-151

Hirschberg J (2001) Carotenoid biosynthesis in flowering plants. Curr Opin Plant Biol **4:** 210-218

Iuchi S, Kobayashi M, Taji T, Naramoto M, Seki M, Kato T, Tabata S, Kakubari Y, Yamaguchi-Shinozaki K, Shinozaki K (2001) Regulation of drought tolerance by gene manipulation of 9-cis-epoxycarotenoid dioxygenase, a key enzyme in abscisic acid biosynthesis in Arabidopsis. Plant J **27:** 325-333

Iuchi S, Kobayashi M, Yamaguchi-Shinozaki K, Shinozaki K (2000) A stress-inducible gene for 9-cis-epoxycarotenoid dioxygenase involved in abscisic acid biosynthesis under water stress in drought-tolerant cowpea. Plant Physiol **123:** 553-562

Kiefer C, Hessel S, Lampert JM, Vogt K, Lederer MO, Breithaupt DE, von Lintig J (2001) Identification and characterization of a mammalian enzyme catalyzing the asymmetric oxidative cleavage of provitamin A. J Biol Chem **276:** 14110-14116

Kohler RH, Cao J, Zipfel WR, Webb WW, Hanson MR (1997) Exchange of protein molecules through connections between higher plant plastids. Science **276:** 2039-2042

Krysan PJ, Young JC, Sussman MR (1999) T-DNA as an insertional mutagen in Arabidopsis. Plant Cell **11:** 2283-2290

Lichtenthaler HK (1999) The 1-deoxy-D-xylulose-5-phosphate pathway of isoprenoid biosynthesis in plants. Annu Rev Plant Physiol Plant Mol Biol **50:** 47-65

Lincoln C, Britton JH, Estelle M (1990) Growth and development of the axr1 mutants of Arabidopsis. Plant Cell **2:** 1071-1080

Lindqvist A, Andersson S (2002) Biochemical properties of purified recombinant human beta-carotene 15,15'-monooxygenase. J Biol Chem **277:** 23942-23948

Mangelsdorf DJ, Kliewer SA, Kakizuka A, Umesono K, Evans RM (1993) Retinoid receptors. Recent Prog Horm Res **48:** 99-121

Markwell J, Bruce BD, Keegstra K (1992) Isolation of a carotenoid-containing sub-membrane particle from the chloroplastic envelope outer membrane of pea (Pisum sativum). J Biol Chem **267:** 13933-13937

McElver J, Tzafrir I, Aux G, Rogers R, Ashby C, Smith K, Thomas C, Schetter A, Zhou Q, Cushman MA, Tossberg J, Nickle T, Levin JZ, Law M, Meinke D, Patton D (2001) Insertional mutagenesis of genes required for seed development in Arabidopsis thaliana. Genetics **159:** 1751-1763

Meza TJ, Stangeland B, Mercy IS, Skarn M, Nymoen DA, Berg A, Butenko MA, Hakelien AM, Haslekas C, Meza-Zepeda LA, Aalen RB (2002) Analyses of single-copy Arabidopsis T-DNA-transformed lines show that the presence of vector backbone sequences, short inverted repeats and DNA methylation is not sufficient or necessary for the induction of transgene silencing. Nucleic Acids Res **30:** 4556-4566

Morris SE, Turnbull CG, Murfet IC, Beveridge CA (2001) Mutational analysis of branching in pea. Evidence that Rms1 and Rms5 regulate the same novel signal. Plant Physiol **126:** 1205-1213

Napoli C (1996) Highly branched phenotype of the petunia dad1-1 mutant is reversed by grafting. Plant Physiol **111:** 27-37

Qin X, Zeevaart JA (1999) The 9-cis-epoxycarotenoid cleavage reaction is the key regulatory step of abscisic acid biosynthesis in water-stressed bean. Proc Natl Acad Sci U S A **96:** 15354-15361

Rameau C, Murfet IC, Laucou V, Floyd RS, Morris SE, Beveridge CA (2002) Pea rms6 mutants exhibit increased basal branching. Physiol Plant **115:** 458-467

Redmond TM, Gentleman S, Duncan T, Yu S, Wiggert B, Gantt E, Cunningham FX, Jr. (2001) Identification, expression, and substrate specificity of a mammalian beta-carotene 15,15'-dioxygenase. J Biol Chem **276:** 6560-6565

Saari JC (1994) Retinoids in photosensitive systems. *In* ABR M.B. Sporn, and D.S. Goodman, ed, The Retinoids: Biology, Chemistry, and Medicine, Ed 2nd. Raven Press, New York, pp 351-385

Schmelz EA, Engelberth J, Alborn HT, O'Donnell P, Sammons M, Toshima H, Tumlinson JH, 3rd (2003) Simultaneous analysis of phytohormones, phytotoxins, and volatile organic compounds in plants. Proc Natl Acad Sci U S A **100:** 10552-10557

Schwartz SH, Qin X, Loewen MC (2004) The biochemical characterization of two carotenoid cleavage enzymes from arabidopsis indicates that a carotenoid-derived compound inhibits lateral branching. J Biol Chem **279:** 46940-46945

Schwartz SH, Qin X, Zeevaart JA (2001) Characterization of a novel carotenoid cleavage dioxygenase from plants. J Biol Chem **276:** 25208-25211

Schwartz SH, Tan BC, Gage DA, Zeevaart JA, McCarty DR (1997) Specific oxidative cleavage of carotenoids by VP14 of maize. Science **276:** 1872-1874

Sessions A, Burke E, Presting G, Aux G, McElver J, Patton D, Dietrich B, Ho P, Bacwaden J, Ko C, Clarke JD, Cotton D, Bullis D, Snell J, Miguel T, Hutchison D, Kimmerly B, Mitzel T, Katagiri F, Glazebrook J, Law M, Goff SA (2002) A high-throughput Arabidopsis reverse genetics system. Plant Cell **14:** 2985-2994

Simkin AJ, Schwartz SH, Auldridge M, Taylor MG, Klee HJ (2004) The tomato CCD1 (Carotenoid Cleavage Dioxygenase 1) genes contribute to the formation of the flavor volatiles β-ionone, pseudoionone and geranylacetone. Plant J **40:** 882-892

Simkin AJ, Underwood BA, Auldridge ME, Loucas HM, Shibuya K, Clark DG, Klee HJ (2004) Circadian regulation of the PhCCD1 carotenoid dioxygenase controls emission of beta-ionone, a fragrance volatile of petunia flowers. Plant Physiol **136:** 3504-3514

Soll J, Schleiff E (2004) Protein import into chloroplasts. Nat Rev Mol Cell Biol **5:** 198-208

Sorefan K, Booker J, Haurogne K, Goussot M, Bainbridge K, Foo E, Chatfield S, Ward S, Beveridge C, Rameau C, Leyser O (2003) MAX4 and RMS1 are orthologous dioxygenase-like genes that regulate shoot branching in Arabidopsis and pea. Genes Dev **17:** 1469-1474

Stirnberg P, Chatfield SP, Leyser HM (1999) AXR1 acts after lateral bud formation to inhibit lateral bud growth in Arabidopsis. Plant Physiol **121:** 839-847

Stirnberg P, van De Sande K, Leyser HM (2002) MAX1 and MAX2 control shoot lateral branching in Arabidopsis. Development **129:** 1131-1141

Sun Z, Gantt E, Cunningham FX, Jr. (1996) Cloning and functional analysis of the beta-carotene hydroxylase of Arabidopsis thaliana. J Biol Chem **271:** 24349-24352

Tan BC, Cline K, McCarty DR (2001) Localization and targeting of the VP14 epoxy-carotenoid dioxygenase to chloroplast membranes. Plant J **27:** 373-382

Tan BC, Joseph LM, Deng WT, Liu L, Li QB, Cline K, McCarty DR (2003) Molecular characterization of the Arabidopsis 9-cis epoxycarotenoid dioxygenase gene family. Plant J **35:** 44-56

Tan BC, Schwartz SH, Zeevaart JA, McCarty DR (1997) Genetic control of abscisic acid biosynthesis in maize. Proc Natl Acad Sci U S A **94:** 12235-12240

Turnbull CG, Booker JP, Leyser HM (2002) Micrografting techniques for testing long-distance signalling in Arabidopsis. Plant J **32:** 255-262

van den Berg H, Faulks, R., Granado, H. F., Hirschberg, J., Olmedilla, B., Sandmann, G., Southon, S., Stahl, W. (2000) The potential for the improvement of carotenoid levels in foods and the likely systemic effects. J Sci Food Agri **80:** 880-912

Van Norman JM, Frederick RL, Sieburth LE (2004) BYPASS1 negatively regulates a root-derived signal that controls plant architecture. Curr Biol **14:** 1739-1746

von Lintig J, Vogt K (2000) Filling the gap in vitamin A research. Molecular identification of an enzyme cleaving beta-carotene to retinal. J Biol Chem **275:** 11915-11920

Ward SP, Leyser O (2004) Shoot branching. Curr Opin Plant Biol **7:** 73-78

Weigel D, Ahn JH, Blazquez MA, Borevitz JO, Christensen SK, Fankhauser C, Ferrandiz C, Kardailsky I, Malancharuvil EJ, Neff MM, Nguyen JT, Sato S, Wang ZY, Xia Y, Dixon RA, Harrison MJ, Lamb CJ, Yanofsky MF, Chory J (2000) Activation tagging in Arabidopsis. Plant Physiol **122:** 1003-1013

Windels P, De Buck S, Van Bockstaele E, De Loose M, Depicker A (2003) T-DNA integration in Arabidopsis chromosomes. Presence and origin of filler DNA sequences. Plant Physiol **133:** 2061-2068

Winterhalter P, Rouseff RL (2002) Carotenoid-derived Aroma Compounds. American Chemical Society : Distributed by Oxford University Press, Washington, DC

Wyatt SE, Kuc, J. (1992) The accumulation of □-ionone and 3-hydroxy esters of □-ionone in tobacco immunized by foliar inoculation with tobacco mosaic virus. Phytopathology **82:** 580-582

Zhao Y, Christensen SK, Fankhauser C, Cashman JR, Cohen JD, Weigel D, Chory J (2001) A role for flavin monooxygenase-like enzymes in auxin biosynthesis. Science **291:** 306-309

Zhao Y, Hull AK, Gupta NR, Goss KA, Alonso J, Ecker JR, Normanly J, Chory J, Celenza JL (2002) Trp-dependent auxin biosynthesis in Arabidopsis: involvement of cytochrome P450s CYP79B2 and CYP79B3. Genes Dev **16:** 3100-3112

BIOGRAPHICAL SKETCH

Michele Auldridge was born in Washington, D.C., on November 7th, 1973. She grew up in Silver Spring, MD, with her parents Michael and Elise, and sister, Laura. Michele graduated from the University of Maryland as a zoology major in 1996 and went on to work as a research assistant for the Biochemistry Department at George Washington University. She then went on to a research technician position at the USDA, making the switch to plants. Michele left the USDA in 2000 to begin her studies at the University of Florida in plant molecular biology.